Are the Chinese Altai "terranes" the result of juxtaposition of different crustal levels during Late Devonian and Permian orogenesis?

Arnaud Broussolle, Min Sun, Karel Schulmann, Alexandra Guy, Carmen Aguilar, Pavla Štípská, Yingde Jiang, Yang Yu, Wenjiao Xiao

Are the Chinese Altai "terranes" the result of juxtaposition of different crustal levels during Late Devonian and Permian orogenesis?

Arnaud Broussolle, Min Sun, Karel Schulmann, Alexandra Guy, Carmen Aguilar, Pavla Štípská, Yingde Jiang, Yang Yu, Wenjiao Xiao

PII: S1342-937X(18)30260-0
DOI: https://doi.org/10.1016/j.gr.2018.11.003
Reference: GR 2039

To appear in: *Gondwana Research*

Received date: 31 May 2018
Revised date: 16 October 2018
Accepted date: 9 November 2018

Please cite this article as: Arnaud Broussolle, Min Sun, Karel Schulmann, Alexandra Guy, Carmen Aguilar, Pavla Štípská, Yingde Jiang, Yang Yu, Wenjiao Xiao , Are the Chinese Altai "terranes" the result of juxtaposition of different crustal levels during Late Devonian and Permian orogenesis?. Gr (2018), https://doi.org/10.1016/j.gr.2018.11.003

Are the Chinese Altai "*terranes*" the result of juxtaposition of different crustal levels during Late Devonian and Permian orogenesis?

Arnaud Broussolle [a], Min Sun [a,*], Karel Schulmann [b,c], Alexandra Guy [b], Carmen Aguilar [b], Pavla Štípská [b,c], Yingde Jiang [d], Yang Yu [d], Wenjiao Xiao [e]

[a] Department of Earth Sciences, The University of Hong Kong, Pokfulam Road, Hong Kong, China

[b] Center for Lithospheric Research, Czech Geological Survey, 11821 Praha 1, Czech Republic

[c] Ecole et Observatoire des Sciences de la Terre, Institut de Physique du Globe de Strasbourg – CNRS UMR7516, Université de Strasbourg, 67084 Strasbourg Cedex, France

[d] State Key Laboratory of Isotope Geochemistry, Guangzhou Institute of Geochemistry, Chinese Academy of Sciences, 510640 Guangzhou, China

[e] State Key Laboratory of Lithospheric Evolution, Institute of Geology and Geophysics, Chinese Academy of Sciences, 100029 Beijing, China

* Corresponding author at: The University of Hong Kong, Department of Earth Sciences, Pokfulam Road, Hong Kong.

E-mail address: minsun@hku.hk (Prof. Min Sun)

Abstract

The general structure of the Chinese Altai has been traditionally regarded as being formed by five tectono-stratigraphic *'terranes'* bounded by large-scale faults. However, numerous detrital zircon studies of the Paleozoic volcano-sedimentary sequences shown that the variably metamorphosed Cambro-Ordovician sequence, known as the Habahe Group, is present at least in four *'terranes'*. It structurally represents deepest rocks unconformably covered by Devonian and Carboniferous sedimentary and volcanic rocks. Calc-alkaline, mostly Devonian, granitoids that intruded all the terranes revealed their syn-subduction related setting. Geochemistry and isotope features of the syn-subduction granitoids have shown that they originated mainly from the melting of youthful sediments derived from an eroded Ordovician arc further north. In contrast, Permian alkaline granitoids, mostly located in the southern part of the Chinese Altai, reflect a post-subduction intraplate setting. The metamorphic evolution of the metasedimentary sequences shows an early MP-MT Barrovian event, followed by two Buchan events: LP-HT mid-Devonian (ca. 400–380 Ma) and UHT-HT Permian (ca. 300–270 Ma) cycles. The Barrovian metamorphism is linked to the formation of a regional sub-horizontal possibly Early Devonian fabric and the burial of the Cambro-Ordovician sequence. The Middle Devonian Buchan type event is related to intrusions of the syn-subduction granitoids during an extensional setting and followed by Late Devonian-Early Carboniferous NE-SW trending upright folding and crustal scale doming during a general NW-SE shortening, responsible for the exhumation of the hot lower crust. The last Permian deformation formed NW-SE trending upright folds and vertical zones of deformation related to the extrusion of migmatites, anatectic granitoids and granulite rocks, and to the intrusions of gabbros and granites along the southern border of the Chinese Altai. Finally, the Permo-Triassic cooling and thrust systems affected the whole mountain range

from ca. 265 to 230 Ma. In conclusion, the Chinese Altai represents different crustal levels of the lower, middle and upper orogenic crust of a single Cambro-Ordovician accretionary wedge, heterogeneously affected by the Devonian polyphase metamorphism and deformation followed by the Permian tectono-thermal reworking event related to the collision with the Junggar arc. It is the interference of Devonian and Permian upright folding events that formed vertical boundaries surrounding the variously exhumed and eroded crustal segments. Consequently, these crustal segments should not be regarded as individual suspect terranes.

Keywords: Central Asian Orogenic Belt, *'Terranes'* in Chinese Altai, Accretionary Complex, Isotopic geochemistry, tectono-metamorphic events

Highlights:

- The Altai is a Cambro-Ordovician volcano-sedimentary accretionary wedge
- The Altai crust differentiated by Devonian melting and sedimentary additions
- The Altai architecture results from Late Devonian to Permian deformation

Contents

1. Introduction

The term *'terrane'* is widely used in modern orogenic research to define a tectono-stratigraphic unit juxtaposed to another one by tectonic processes along a convergent boundary (Coney et al., 1980). However, during last decades this term has been overused or even misinterpreted because of the wrong interpretation of the lithostratigraphy or the nature of boundaries between different tectonic units (Sengör and Dewey, 1990). According to the original definition, terranes must be delimited by distinct boundaries (faults, sutures) that separate units with different stratigraphy, deformation pattern, metamorphism, etc (Dewey, 1977; Coney et al., 1980). In the most favourable cases, the presence of an ophiolite belt can clearly mark an oceanic suture between different blocks (Dewey, 1977). Recently, a range of techniques has been used to discriminate different terranes in orogens such as the lithostratigraphy combined with the biostratigraphy (e.g. Badarch et al., 2002), involving studies of detrital zircon spectra, ages and the nature of metamorphism and geophysical characteristics (e.g. Guy et al., 2014b). Indeed, terranes defined by the above mentioned methods can be genetically linked to the original mother continent by their distinct geological archive, geophysical signature or paleontological record (Coney et al., 1980; Xiao et al., 2015). Subsequently, these blocks with distinct characteristics and evolution can be later juxtaposed along a tectonic boundary (subduction-collisional zone, transform or strike slip faults) to a different tectonic domain with a completely different geological record. However, as mentioned above, the assembled two units along a convergent boundary can be heterogeneously reworked (by magmatism, metamorphism and

deformation) and the whole zone can provide a false image that can be interpreted as an assembly of exotic terranes. Such a misunderstanding of the tectonic settings of different units is common in literature and may lead to a huge proliferation of terranes in particular in the accretionary systems (e.g. Badarch et al., 2002).

1.1. Overview of the CAOB and the Chinese Altai

The Central Asian Orogenic Belt (CAOB) is a giant accretionary orogen extending from the Siberian craton in the north to the Tarim and North China cratons in the south, which may have evolved from ca. 600 to 230 Ma (Fig. 1 inset; Mossakovsky et al., 1993; Şengör et al., 1993; Şengör and Natal'in, 1996; Windley et al., 2007; Xiao et al., 2010; Eizenhöfer et al., 2014). The CAOB is formed by the accretion of continental blocks of different origin, accretionary complexes, island arcs and back arcs (Jahn et al., 2000a, 2004; Xiao et al., 2015). Wilhem et al. (2012) divided the CAOB in the Peri-Siberian, Kazakhstan and Tarim-North China tectonic domains based on their affinity to the continental masses during Paleozoic. The Peri-Siberian domain is also called the Mongolian collage (Xiao et al., 2015). It outcrops mainly in Mongolia, eastern Kazakhstan, northern China and southern Russia and includes microcontinental blocks of Grenville age (Rojas-Agramonte et al., 2011), Proterozoic to Paleozoic oceanic fragments and accretionary wedges of various ages (Fig. 1). Almost the complete association of tectonic units occurs in Mongolia, where it was characterized into seven types of tectonic domains (cratonal, metamorphic, passive margin, island arc, forearc/backarc, accretionary complex, ophiolite) formed of 44 different terranes (Badarch et al., 2002). This model implies complex amalgamation of blocks associated with the emplacement of numerous ophiolitic fragments along multiple sutures (e.g. Xiao et al., 2009). However, this complex classification of Mongolia (Badarch et al., 2002) is questioned by recent studies, that suggest a continuous evolution of the

whole accretionary system during Paleozoic times above one single giant subduction zone (Buriánek et al., 2017; Jiang et al., 2017; Janoušek et al., 2018).

Figure 1 Map of Mongolian collage about here

The key element of the Mongolian collage is the 2000 km long Altai orogenic belt extending from Russia, Kazakhstan, Mongolia and northern China and rimming the southern margin of the Tuva-Mongol, Zavkhan, Baydrag and Erguna microcontinental blocks (Fig. 1). The Chinese Altai forms a 400 km long southern part of this belt and represents its most extensively studied area. The Chinese Altai was divided into five tectono-stratigraphic terranes and was considered to be the lateral continuity with the Mongolian terranes defined further east (Windley et al., 2002; Xiao et al., 2004). More than a decade has passed since the terranes were defined in Mongolia and China, and significant amount of geological, geophysical and geochemistry data are now available enabling to test the nature of the suspect terranes in the Chinese Altai. In particular, volcano-sedimentary sequences forming the Chinese Altai were widely examined in detail using a U–Pb dating of detrital zircons and their Hf isotopic signature. All these data brought new ideas about the provenance and the tectonic settings of different volcano-sedimentary sequences forming the Chinese Altai (Long et al., 2008, 2012; Sun et al., 2008; Jiang et al., 2011). The magmatic rocks were also extensively studied using geochemistry, isotopic methods and geochronology, which revealed the nature of granitoids, the source of parental magmas and their tectonic settings (Jahn et al., 2000a; Chen and Jahn, 2002; Yuan et al., 2007; Wang et al., 2009a; Cai et al., 2011c; Liu et al., 2012). Several modern metamorphic studies showed a contrasting timing of the thermal and baric evolution across the whole orogenic belt (Zhuang, 1994; Wei et al., 2007; Jiang et al., 2010; Tong et al., 2014a; Jiang et al., 2015). Even structural studies mostly focused on the Late Paleozoic Erqis shear zone, which separates

the Chinese Altai from the southerly Junggar arc (Laurent-Charvet et al., 2002, 2003; Briggs et al., 2007; Zhang et al., 2012; Li et al., 2015a), and few structural studies carried out in the interior parts of the Chinese Altai revealed pivotal information for the Early Paleozoic evolution of the whole Altai orogenic belt (Zhang et al., 2015; Li et al., 2016b; Broussolle et al., 2018). Altogether, these data can be now assembled in a multi-disciplinary review correlating and synthetizing all the previous work in the Chinese Altai. In this paper, we will focus on a review of the stratigraphy, magmatism, metamorphic and deformation history of the Chinese Altai, in order to show that the distinction of the supposed terranes is not appropriate for this area. In contrast, the rock association in the Chinese Altai can be seen as a coherent accretionary wedge heterogeneously reworked by subduction and collision processes, which can be extrapolated to the whole Altai orogenic belt extending across Russia, Kazakhstan and Mongolia.

1.2. Review of the supposed terranes in the Chinese Altai

Windley et al. (2002) identified five distinct terranes resulting from the juxtaposition of units marked by distinct stratigraphy, metamorphism and deformation pattern along steep faults (Fig. 2). Here, we provide a short lithostratigraphical characterization of the individual terranes and the nature of their boundaries: the North Altaishan, the Northwest Altaishan, the Central Altai, the Qiongkuer-Abagong and the South Altaishan terranes (Fig. 2). The North Altaishan terrane, located in the eastern part of the Chinese Altai (terrane 1 in Fig. 2), is composed of Middle Devonian to Early Carboniferous clastic sediments and limestones intercalated with volcanic rocks that are grouped in the Altai and Kalaerqisi formations, respectively. This terrane is supposedly delimited from the Central Altai terrane by the Hongshanzui-Kurekete normal fault (Liu et al., 2012). The Northwest Altaishan terrane in the northern part of the Chinese Altai (terrane 2 in Fig. 2) is mainly composed of Cambro-Ordovician turbiditic volcanoclastic

sequences forming the Habahe Group. This terrane is also composed of the Dongxileke and Baihaba formations, which represent a minor Devonian volcanic suite and a Cambro-Ordovician marine-facies sedimentary sequence, respectively (Long et al., 2012). The Central Altai terrane, located in the central to southeastern part of the Chinese Altai (terrane 3 in Fig. 2), is mainly composed of presumably Neoproterozoic to Silurian sediments of the Kulumiti Formation. This formation is lithologically similar to the Cambro-Ordovician Habahe Group that forms bulk of the Northwest Altaishan terrane. The Central Altai is delimited from the southerly Qiongkuer-Abagong terrane by the Abagong-Kuerti fault (Liu et al., 2012), known also as Barils thrust (The Team One of Geology of Xinjiang, 1979; Yang et al., 2011). The Qiongkuer-Abagong terrane is a narrow NW-SE trending belt (terrane 4 in Fig. 2) mainly formed by the Early Devonian Kangbutiebao and Middle Devonian Altai formations, which represent a volcano-sedimentary and turbiditic sequence, respectively (Windley et al., 2002). However, the southern extremity of the Qiongkuer-Abagong terrane was recently described as a volcano-sedimentary sequence that belongs to the Cambro-Ordovician Habahe Group (see Fig. 1; Yang et al., 2011; Liu et al 2012; Zhang et al., 2012). The Qiongkuer-Abagong terrane is delimited from the South Altaishan terrane by the Kezijiaer-Tesibahan fault (Liu et al., 2012), known previously as Altai-Qinghe fault (The Team One of Geology of Xinjiang, 1979; Yang et al., 2011). The South Altaishan terrane is composed of schist and high-grade gneiss (terrane 5 in Fig. 2), both of which are overlain tectonically by the Devonian Altai and Late Carboniferous Kalaerqisi sedimentary rocks. This terrane is similar to the North Altaishan terrane in term of lithology (Windley et al., 2002). The South Altaishan terrane is delimited from the Junggar island arc system by the Erqis fault (Li et al., 2015a), which is assumed to be one of the largest transcurrent faults in the Central Asia (He, 1990; Şengör et al., 1993). The Erqis fault zone contains fragments of Devonian

ophiolitic rocks and therefore is considered to constitute a suture between the Junggar arc system and the Chinese Altai orogenic belt (Wang et al., 2003). The Chinese Altai was also divided into five different terranes by Xiao et al. (2004) in continuity with terranes defined previously in Mongolia (Badarch et al., 2002). However, in this paper we will use the terms and numbers of the originally defined terranes by Windley et al. (2002).

Figure 2 Map of Chinese Altai about here

One of the main criteria allowing the identification of suspect terranes is their geophysical characteristics, in particular gravity and magnetic signatures because these signals depend on the petrophysical properties (density and magnetic susceptibility) of the constituent rocks. The gravity signal of the Mongolian and Chinese Altai was evaluated by Guy et al. (2014b, 2015) and Jiang et al. (2016). These authors showed that both the Chinese and Mongolian Altai display a rather homogeneous gravity signal unlike other accretionary belts, where distinct terranes reveal highly contrasting gravity signal (e.g. Alaska and Tasman belt; Glen et al., 2007; Burton, 2010). Here, we explore this issue further and present the Bouguer anomaly data from the NW China that were extracted from the Earth Global Model 08 (EGM08) and are available at a spatial resolution of 2.5×2.5 arc minute. EGM08 combines terrestrial, altimetry-derived, airborne gravity data and gravitational information derived from the topography over areas with lower resolution gravity data (Pavlis et al., 2012). The Bouguer gravity anomaly map has been obtained using a mean crustal density of 2670 kg/m^3. The Bouguer anomalies range from −310 mGal to −80 mGal and reveal two principal domains delimited by one main NW-SE trending gradient, with a broad gravity low which correlates with the Mongolian Altai in the north, and a prominent gravity high corresponding to the Junggar arc in the south (Fig. 3). The Chinese Altai is at the transition between the gravity high and the gravity low. The most prominent feature is lack of

any geophysical boundary correlating with limits of the suspect terranes as they have been previously defined in the Chinese Altai (Fig. 3). It is in particular the lack of correlation between the Erqis fault and the boundary of the main gravity high which defines the extent of the Junggar arc. The low-frequency gravity highs in the central part of the Chinese Altai also show no correlation with the North Altaishan and Central Altai terranes. The lack of any possible correlation of the terrane boundaries with gravity signal calls for discussion and explanation.

Fig 3 map of gravity about here

2. Sedimentary record in the Chinese Altai

2.1. Distribution and ages of detrital sediments

When fossils are missing or sedimentary rocks are highly deformed and metamorphosed, the age and provenance of sedimentary sequences are constrained by studying detrital zircons (Fedo et al., 2003; Gehrels, 2012). The Chinese Altai is mainly composed of three distinct Paleozoic volcano-sedimentary sequences that have been extensively studied during the last decade (supplementary material S1 and references therein): the Cambro-Ordovician sequence composed of the Habahe Group, the Kulumiti and the Baihaba formations, the Devonian sequence composed of the Kangbutiebao and the Altai formations, and the Carboniferous Kalaerqisi sequence (see Fig. 4).

2.1.1. The Cambro-Ordovician sequence

The Cambro-Ordovician sequence is 4000 to 6000 m thick and mainly consists of the Habahe Group and the Kulumiti Formation, and the Baihaba Formation, which is locally distributed (Figs. 2, 4 and 5). This sequence primarily constitutes the Northwest Altaishan and Central Altai

terranes and is composed of sandstone, siltstone, shale and locally limestone, metamorphosed from sub-greenschist to amphibolite facies (Long et al., 2007; Cai et al., 2011a; Wang et al., 2014c; Jiang et al., 2015). Late Ordovician age was proposed based on (*Plasmoporella sp., Propora sp., Palaeophyllum sp., and Madiolopsis sp.*) fossils found in limestones of the upper level of the Baihaba Formation, which unconformably overlies the Habahe Group in the Northwest Altaishan terrane (Fig. 4) (see Windley et al., 2002 for summary).

Figure 4 stratigraphy about here

The detrital zircon patterns of the metasediments from the Northwest Altaishan, Central Altai and Qiongkuer-Abagong terranes have a youngest peak in Ordovician at ca. 465 Ma and a major peak in Cambrian around 500 Ma with inherited Precambrian grains (see Table S1; Long et al., 2007; Sun et al., 2008; Long et al., 2010; Jiang et al., 2010, 2011; Yang et al., 2011; Wang et al., 2014c; Zhang et al., 2015; Broussolle et al., 2018). In addition, in the southeastern part of the South Altaishan terrane, a paragneiss sample yields a youngest zircon population at Early Ordovician (ca. 472 Ma) with few Proterozoic ages (between ca. 817 to 2251 Ma; Zhang *et al.*, 2012), showing that this sample is a metamorphic equivalent of the Habahe Group exposed in other terranes. The youngest peaks (ca. 438 Ma and 465 Ma) indicate that all the maximum depositional age of these rocks is in the Middle to Late Ordovician. Wang et al. (2014c) dated two metasedimentary samples from the Kulumiti Formation in the Central Altai terrane and obtained a mean zircon population around 464–576 Ma, with a major peak at ca. 510 Ma and a youngest peak at ca. 465 Ma, and inherited Precambrian grains. Consequently, the maximum depositional age was constrained at ca. 465 Ma similar to the Ordovician Habahe Group (Fig. 5). Taken together, these findings support the close relationship between the Kulumiti Formation and the Habahe Group in the Central Altai (Wang et al., 2014c). However, zircons from a

metarhyolite interlayered in this Cambro-Ordovician sedimentary sequence yield an eruption age of ca. 502 Ma (Yang et al., 2011) indicating that the sedimentation time of Habahe Group can be even older than 500 Ma, which is the age corresponding to the major Late Cambrian detrital zircon peak.

All these data are now summarized in probability density plots (Fig. 5) for four different terranes. The Northwest Altaishan probability density plot yields a major peak in Cambrian around 495 Ma, and minor peaks in Neoproterozoic around 801 Ma and in Paleoproterozoic around 1984 Ma (Long et al., 2007; Sun et al., 2008: Long et al., 2010; Jiang et al., 2010, 2011). From the Central Altai, the detrital zircon analyses provide a major peak in Cambrian around 504 Ma, and minor peaks in Neoproterozoic around 795 Ma and in Paleoproterozoic around 1994 Ma (Long et al., 2007; Jiang et al., 2011; Wang et al., 2014c). The Qiongkuer-Abagong probability density plot yields a major peak in Cambrian around 514 Ma with inherited grains in Neoproterozoic of ca. 793 Ma and in Paleoproterozoic of ca. 2004 Ma (Long et al., 2007; Sun et al., 2008; Yang et al., 2011; Zhang et al., 2015; Broussolle et al., 2018). Taken together, the probability density plots for the Northwest Altaishan, Central Altai and the Qiongkuer-Abagong terranes show that the sedimentary sequences are similar and therefore the stratigraphy of these terranes is identical. In addition, the geochemical data clearly suggest an active continental margin environment for all these volcano-sedimentary rocks (Long et al., 2008; Jiang et al., 2016), further supporting the above interpretation.

Figure 5 detrital map about here

2.1.2. The Devonian sequence

The Devonian sequence is composed of the volcano-clastic Kangbutiebao and turbiditic Altai formations, respectively (Windley et al., 2002; Cai et al., 2011a). The 4000–5000 m thick

Kangbutiebao Formation unconformably overlies the Cambro-Ordovician sequence and is composed of sedimentary and volcano-clastic rocks, which underwent greenschist to amphibolite facies metamorphism (Fig. 4). The volcanic rocks of the Kangbutiebao Formation yielded U–Pb zircon ages ranging from ca. 396 to 421 Ma (see Table S1; Zhang et al., 2000; Chai et al., 2009; Liu et al., 2010; Shan et al., 2011; Wan et al., 2011; Chai et al., 2012; Geng et al., 2012; Liu et al., 2012; Guo et al., 2015; Yang et al., 2017). Long et al. (2007) obtained a detrital pattern for a mylonite from the Kangbutiebao Formation with the youngest zircon population in Early Silurian at ca. 432 Ma. This sample is also composed of Early Paleozoic detrital zircons giving a major peak in Late Cambrian at ca. 501 Ma (Long et al., 2007), suggesting that the sedimentary source for the Habahe Group possibly also supplied significant materials.

The overlaying Altai Formation is 6000 m thick and is distributed in the North Altaishan, Qiongkuer-Abagong and South Altaishan terranes (Fig. 2). The formation is mostly composed of volcanic rocks, marine clastic sediments, limestone, marble and highly deformed paragneiss and migmatites (Jiang et al., 2015). Based on numerous fossils preserved in limestone horizons (*Cymostrophia cf. stephani, Cymostrophia aff. guadrata, Megastrophia sp., Stropheodonta sp., Euryspirifer sp., Acrospirifer sp., Brachyprion sp., Cyrtospirifer, sp., Favosites goldfussi, Pachyfavosites palymorphus, Pachyfavosites yui, Pachyfavosites vilvaensis, Calceola sandalina subsp. Sinensis*), a Middle-Devonian age of the Altai Formation was proposed (see Windley et al., 2002 for summary). Unfortunately, zircon U–Pb age data are unavailable up to date for the Altai sediments from the North Altaishan and the South Altaishan terranes. Only a recent U–Pb zircon dating from a felsic intra-formational volcanic rock in the Kalasu area of the Qiongkuer-Abagong terrane yields 388 ± 1 Ma U–Pb age, confirming the Middle Devonian age for this formation (Broussolle et al., 2018). However, the detrital zircons from schists and paragneisses

from this unit show an age pattern similar to that for the Cambro-Ordovician sequence, indicating that Devonian detrital zircons are absent in medium- to high-grade metamorphic rocks of the Qiongkuer-Abagong terrane (see Table S1; Long et al., 2007; Jiang et al., 2010; Shan et al., 2011; Zhang et al., 2012; Tong et al., 2013; Broussolle et al., 2018).

According to the geological map, the Qiongkuer-Abagong terrane is almost completely composed of the Altai Formation (Figs. 2 and 5). The high-grade rocks of the Qiongkuer-Abagong terrane are either Devonian intrusions or more often metamorphosed Cambro-Ordovician sediments (see Table S1; Long et al., 2007; Sun et al., 2008; Jiang et al., 2010; Tong et al., 2013; Zhang et al., 2015; Broussolle et al., 2018), as shown by numerous Late Cambrian and Ordovician detrital zircon ages from paragneisses and migmatites. In conclusion, the extent of the Altai Formation was largely overestimated by previous studies, probably due to the presence of high-grade gneisses and migmatites that were not dated.

2.1.3. The Carboniferous sequence

The Carboniferous sequence, called Kalaerqisi Formation, is found in the North Altaishan and South Altaishan terranes and is 5000 to 7000 m thick (BGMRX, 1978). The sequence in the North Altaishan terrane is composed of interbedded siliceous and argillaceous slate, siltstone and highly deformed tuff (Windley et al., 2002; Liu et al., 2012) (Fig. 4). Unfortunately, zircon U–Pb age data are unavailable up to date for the sediments from the North Altaishan terrane but fossils preserved in limestones layers (*Barrandeophyllum sp., Eopteria ? sp., Lunulacardium ? sp., and Cyclocyclicus ? sp.*) suggest that it is Early Carboniferous in age (see Windley et al., 2002 for summary). The Carboniferous sequence in the South Altaishan terrane contains slate, schist and gneiss metamorphosed in amphibolite facies (Chen and Jahn, 2002; Li et al., 2015a, 2016a, 2017). Although the sequence still contains detrital zircons of Cambrian and Ordovician ages,

the depositional age of the sequence was defined as Middle Carboniferous (ca. 322–326 Ma) based on detrital U–Pb zircons from two schist samples of the Erqis shear zone (Li et al., 2015a) (Fig. 5 and Table S1).

2.2. Epsilon Hf data for the detrital zircons from the Chinese Altai

A database of 639 available Hf-in-zircon analyses for metasediments was established in order to compare the distribution of their hafnium values according to the different terranes (Fig. 6). The total of available data consist of 423 analyses for the Northwest Altaishan, 87 analyses for the Central Altai, 88 analyses for the Qiongkuer-Abagong and 41 analyses for the South Altaishan terrane (see Table S1; Long et al., 2007, 2010; Sun et al., 2008; Jiang et al., 2011; Li et al., 2017). Unfortunately, no data are available for the North Altaishan terrane. Five clusters can be distinguished in the epsilon $Hf_{(t)}$ versus age diagram for detrital zircon (Fig. 6): (1) Archean to Paleoproterozoic, (2) Mesoproterozoic, (3) Neoproterozoic, (4) Cambrian to Silurian and (5) Devonian to Carboniferous.

Figure 6 detrital Hafnium isotopes about here

Archean to Paleoproterozoic zircons (ca. 1500 to 2900 Ma) have mostly negative ε_{Hf} (t) values ranging from +4 to -25 and are possibly derived from the Tuva-Mongol, Baydrag and Zavkhan microcontinental blocks to the north as proposed by Jiang et al. (2011, 2017). Importantly, the zircon ε_{Hf} (t) patterns are the same for the Northwest Altaishan, Central Altai and Qiongkuer-Abagong terranes, implying that these terranes had the same tectonic setting and received the same sediment supply. The Mesoproterozoic detrital zircons (ca. 1000 to 1500 Ma) have positive ε_{Hf} (t) values ranging from 0 to +19. The source of these zircons cannot be well

defined due to the lack of data for the Mesoproterozoic rocks in Mongolia (Fig. 6). Neoproterozoic zircons (ca. 600 to 900 Ma) have negative to positive ε_{Hf} (t) values ranging from -24 to +10 (Fig. 6). Previous researchers suggested that the Neoproterozoic ophiolites were formed in a 570 Ma intra-oceanic arc and then emplaced in an accretionary wedge (Kovach et al., 2011; Buriánek et al., 2017). Dioritic and tonalitic rocks with Grenvillian age (ca. 800–900 Ma) and positive ε_{Hf} (t) values intruded the Mesoproterozoic Baydrag and Zavkhan continents (Bold et al., 2016; Buriánek et al., 2017; Janoušek et al., 2018). These ophiolitic and acidic rocks may provide zircons with positive ε_{Hf} (t) values to the Chinese Altai. In addition, some Neoproterozoic granitoids with negative ε_{Hf} (t) values are also exposed in the region (Buriánek et al., 2017). They may provide zircons with negative ε_{Hf} (t) values to the Chinese Altai. The Cambrian to Silurian cluster displays positive and negative epsilon Hf values, suggesting that the source of their precursor Early Paleozoic magmas included both juvenile and old materials (Long et al., 2007; Jiang et al., 2011) or that their provenance contained Paleozoic igneous rocks with different origins (Long et al., 2012; Jiang et al., 2017). One possible source for the juvenile Cambro-Ordovician zircons are the Late Cambrian to Ordovician granitoids intruding the Proterozoic ophiolites of the Lake zone (North East of the Altai Range) and underlying the Precambrian basement (Janoušek et al., 2014, 2018; Jiang et al., 2016). In that region, the giant Ikh-Mongol arc granitoids of Late Cambro-Ordovician age intruded the southern margin of the Precambrian continental blocks (namely the Tuva-Mongol, Baydrag and Zavkhan blocks). The presence of the Proterozoic ophiolites on their margins indicate accretion of oceanic rocks in the Proterozoic (Kovach et al., 2011; Yarmolyuk et al., 2011; Buriánek et al., 2017; Soejono et al., 2017). Negative epsilon Hf values are recorded in the Cambro-Ordovician sequence and interpreted as reflecting magmatic recycling of the Precambrian basement rocks of the Ikh-

Mongol arc (Jiang et al., 2017). All that implies that the Lake zone and the Tuva-Mongol, Baydrag and Zavkhan microcontinental blocks rocks were massively eroded during Ordovician. The Devonian to Carboniferous cluster displays positive epsilon Hf values, which show a juvenile affinity (Li et al., 2017). The source of those detrital grains is mostly the eroded Devonian to Carboniferous granitoids of the Chinese Altai with Cambro-Ordovician inherited grains.

3. Distribution and geochemistry of the granitoids in the Chinese Altai

The Paleozoic magmatic rocks cover nearly 40% of the Chinese Altai and their juvenile isotopic signature has been interpreted to reflect a massive crustal growth during Paleozoic (Jahn et al., 2000b; Chen and Jahn, 2002). The ages and the compositions of these granitoids rocks can provide essential information to constrain the crustal evolution and timing of tectono-magmatic processes. In this section, we synthesize available U–Pb age (Fig. 7), major element geochemistry (Fig. 8), whole-rock Hf and Nd (Fig. 9) and Hf-in-zircon isotopic compositions (Fig. 10). This enables us to investigate whether there are geochemical and isotopic differences for the granitoid intrusions in the individual terranes. The data used for this section can be found in the Tables S2, S3, S4, S5 and S6 of the supplementary material.

3.1. Magmatic events in the Paleozoic

The available U–Pb zircon ages for the granitoids show a dominant Early to Middle Paleozoic magmatic event and a less prominent Permian magmatic event (Fig. 7). Early to Middle Paleozoic granitoids (ca. 507–310 Ma) show I- to S-type affinities (Wang et al., 2006; Yuan et al., 2007; Sun et al., 2008; Wang et al., 2009a; Cai et al., 2011c; Zhang et al., 2017a) and are

interpreted as syn-subduction granitoids. Several studies showed that the magmatism was rather continuous from ca. 507 to 360 Ma (Fig. 7) with a major peak at around 400 Ma (see Table S2; e.g. Lou, 1997; Yuan et al., 2001; Chen and Jahn, 2002; Windley et al., 2002; Hong et al., 2003 Tong et al., 2005, 2007; Yuan et al., 2007; Sun et al., 2008, 2009; Cai et al., 2011a,b,c Yang et al., 2011; He et al., 2015) and that the latest syn-subduction granitoids are recorded at ca. 330 to 313 Ma (Chen and Jahn, 2002; Yuan et al., 2007; Kozavok et al., 2011; Cai et al., 2012a). Early Paleozoic granitoids are metamorphosed and transformed to strongly foliated orthogneiss (Wang et al., 2009a). Permian A- to S-type granitoids (ca. 290 to 250 Ma) show more alkaline composition, mainly intruded the Central Altai, Qiongkuer-Abagong and South Altaishan terranes, are mostly circular in shape and undeformed (Fig. 7). They are considered as post-subduction, formed after the collision of the Chinese Altai arc and the Junggar arc system (Tong et al., 2014b; and references therein).

All the U–Pb zircon data for these granitoids are now summarized in probability density plots (Fig. 7) for five different terranes. The granitoids in the North Altaishan show Devonian zircon population from 396 to 412 Ma with a peak at ca. 400 Ma, implying that the Devonian sediments intruded by these granitoids should be older than ca. 412 Ma (Lou, 1997; Yuan et al., 2001). Some granitoids already intruded the Northwest Altaishan terrane in the Ordovician but granitoids were mostly emplaced in the Devonian in this terrane (ca. 410–380 Ma; Chen and Jahn, 2002; Tong et al., 2005, 2007; Sun et al., 2009; Jiang et al., 2010; Cai et al., 2011a,b). Granitoids intruded the Central Altai and Qiongkuer-Abagong terranes from the Late Cambrian to Jurassic, but the main magmatic pulse was around 400 Ma (Wang and Zhao, 1998; Chen and Jahn, 2002; Windley et al., 2002; Hong et al., 2003; Zhang et al., 2003; Tong et al., 2005; Wang et al., 2006; Zhu et al., 2006; Tong et al., 2007; Yuan et al., 2007; Liu et al., 2008; Sun et al.,

2008; Wang et al., 2009a; Cai et al., 2010; Gao et al., 2010; Yang et al., 2010; Zhang et al., 2010; Cai et al., 2011a,c; Kozakov et al., 2011; Yang et al., 2011; Cai et al., 2012a; Wang et al., 2014a; Zheng et al., 2016 ; Zhang et al., 2017a). The available data show a rather important Ordovician magmatic peak (ca. 448–451 Ma) for the South Altaishan terrane, with other two important peaks in Devonian (ca. 420–380 Ma) and Permian (ca. 290–250 Ma) (Zhang et al., 2006; Briggs et al., 2007; Yuan et al., 2007; Zhou et al., 2007; Sun et al., 2009; Li et al., 2012; Tong et al., 2012; Zhang et al., 2012; Wan et al., 2013; Tong et al., 2014b; He et al., 2015; Zhang et al., 2015). In conclusion, the synthesis of zircon age data shows that syn-subduction granitoids in the Chinese Altai are evenly distributed over the five terranes, whereas post-subduction granitoids are locally dispersed along two narrow NW-SE trending terranes located in the southern Chinese Altai (Fig. 7). The presence of Late Cambrian to Ordovician granitoids implies that the volcano-sedimentary sequence intruded by these granitoids can be in some places older than ca. 507–448 Ma (Wang et al., 2006; Liu et al., 2008; Sun et al., 2009; Cai et al., 2011a,c; Zhang et al., 2017a). Unfortunately, only few detrital zircon data linked to the sedimentary environment are available for almost all the region to get a better constrain of the tectono-sedimentary evolution of the whole system through time.

Figure 7 granitoids map about here

3.2. Geochemistry of the Cambrian to Carboniferous granitoids

In this work we summarize analyses for the Northwest Altaishan (n=20), Central Altai (n=66), Qiongkuer-Abagong (n=46) and South Altaishan (n=16) terranes (see Table S3; Chen and Jahn, 2002; Zhang et al., 2003; Zhang et al., 2006; Zhu et al., 2006; Yuan et al., 2007; Sun et al., 2009; Yang et al., 2010; Cai et al., 2011b, 2012b; Yu et al., 2017; Zhang et al., 2017a). The

Cambrian to Carboniferous granitoids can be considered as typical Tonalite-Trondjemite-Granodiorite (TTG) suite, which implies their syn-subduction origin (Yuan et al., 2007; Cai et al., 2011c; Liu et al., 2012 and references therein). On the Na_2O+K_2O vs SiO_2 diagram, the samples from the Chinese Altai granitoids cluster in the granite and granodiorite fields with high SiO_2 content (Fig. 8a; 62–78 wt.% SiO_2). Some samples from the Qiongkuer-Abagong terrane define as tonalite cluster in the diorite field with medium SiO_2 (57–61 wt.%; Yuan et al., 2007). Few samples of mafic enclaves cluster in the gabbro and syeno-diorite fields with low SiO_2 content from 52 to 54 wt.% (Cai et al., 2012a). The data show that there is no systematic compositional variation according to the different terranes. The A/NK - ASI diagram shows that the granitoids from the four terranes plot in the metaluminous to peraluminous fields and are evenly distributed irrespective to the terrane classification (Fig. 8b). The K_2O - SiO_2 diagram (Fig. 8c) show that most of the studied granitoids from the four terranes correspond to high-K calc-alkaline to calc-alkaline associations, with some falling in the shoshonitic and tholeiitic fields. The K_2O versus SiO_2 diagram shows that there is a slight difference among different terranes but not significant enough to assert different tectonic settings. On the Fe_2O_3*5-(Na_2O+K_2O)-(MgO+CaO)*5 ternary diagram (Fig. 8d), based on the molecular quantities of rock-forming oxides, the samples of the Chinese Altai granitoids cluster outside of the recognized fields of A-type rocks (corresponding to silicic rocks of within-plate geodynamic settings (A_1) and felsic igneous rocks associated with intracontinental and continental-margin geodynamic settings (A_2); Grebennikov, 2014). This fact indicates that all the syn-subduction granitoids in the Chinese Altai correspond to S- and I-type felsic igneous rocks of major geodynamic settings (e.g. zones of magmatism of active continental margins, involving continental crust in magma formation; Jiang et al., 2016). In summary, the syn-subduction

granitoids in the Chinese Altai have similar chemical compositions regardless of different terranes.

Figure 8 geochemistry about here

3.3. Isotopic features of the Cambrian to Carboniferous granitoids

Because Nd-Hf isotopes are decoupled in the Chinese Altai (Yu et al., 2017), it is important to study both isotopes separately in order to compare the whole-rock ε_{Hf} (t) with the whole-rock ε_{Nd} (t) data (Fig. 9a, b). Whole-rock Lu-Hf data have been calculated for Devonian granitoids from the Chinese Altai with 7 data from the Northwest Altaishan terrane, 3 data from the Central Altai terrane and 7 data from the Qiongkuer-Abagong terrane (see Table S4 in supplementary material). The ε_{Hf} (t) values are positive, ranging from +2 to +13, which could imply the importance of juvenile mantles in the magma source in the Chinese Altai irrespective of the terranes (Fig. 9a).

Whole-rock Sm-Nd isotopic values for the Cambro-Carboniferous granitoids cover four terranes (see Table S5 in supplementary material): the Northwest Altaishan (n=20), Central Altai (n=61), Qiongkuer-Abagong (n=42) and South Altaishan (n=12) terranes (Zhao et al., 1993; Chen and Jahn, 2002; Zhou et al., 2005; Yuan et al., 2007; Wang et al., 2009a; Cai et al., 2011b; Tong et al., 2012; Yu et al., 2017; Zhang et al., 2017a). Cambrian to Carboniferous granitoids show positive to negative whole-rock ε_{Nd} (t) (-11 to +8). Samples from the Northwest Altaishan terrane have mostly negative ε_{Nd} (t) values spanning from -4 to 0 for the 412–390 Ma old granitoids (see Fig. 9b and Table S5). Samples from the Central Altai and Qiongkuer-Abagong terranes have negative to positive ε_{Nd} (t) values ranging from -11 to +6 for the 507–318 Ma old

granitoids (Fig. 9b and Table S5). Samples from the South Altaishan terrane have positive ε_{Nd} (t) values spanning from +2 to +8 for the 400–330 Ma old intrusions (Fig. 9b and Table S5). The variations of the ε_{Nd} (t) values show a younging T_{DM} (crustal model ages) trend from northeast to southwest: the Northwest Altaishan and Central Altai terranes were characterized by T_{DM} model ages from 1100 to 1600 Ma, the Qiongkuer-Abagong terrane by T_{DM} model ages of ca. 800–1600 Ma and the South Altaishan terrane by T_{DM} model ages from 500 to 1000 Ma (see Table S5; Zhao et al., 1993; Chen and Jahn, 2002; Zhou et al., 2005; Yuan et al., 2007; Wang et al., 2009a; Cai et al., 2011b; Tong et al., 2012; Zhang et al., 2017a). Therefore when separating the syn-subduction from the post-subduction granitoids, only the South Altaishan terrane has distinguishable positive Nd values, which imply a younger T_{DM} model age (Fig. 9b). These Nd isotopic values show mostly juvenile characteristics suggesting the dominance of juvenile materials in the magma source. Liu et al. (2012) separated the Chinese Altai syn-subduction granitoids into two groups with ε_{Nd} (t) lower than +1 and ε_{Nd} (t) higher than +1, and concluded that some of the granitoids are formed by re-melting of a continental crust and others are formed by mantle derived melt respectively. This interpretation may apply to granitoids with negative to positive ε_{Nd} (t) values (-10 to +6), which occur in the Northwest Altaishan, Central Altai and Qiongkuer-Abagong terranes (Fig 9b). A study of the syn-subduction granitoids demonstrates that both reworking of the Precambrian crust and interaction with the mantle magma can account for the mixed Nd isotopic signature (Liu et al., 2012). In contrast, Jiang et al. (2016) showed that the close temporal and spatial relationship between the regional anatexis of the Habahe Group volcano-sedimentary rocks and the formation of granitoids, as well as their geochemical similarities including un-evolved Nd isotopic signatures, the enrichment of Large Ion Lithophile

Elements relative to many of the High Field Strength Elements is indicative for the Pacific type magmatism resulting from the partial melting of the accretionary wedge rocks.

Figure 9 Hf and Nd isotopes about here

Single grain isotopic composition can give additional evidence to decipher the source of the granitoids. In this section we present 613 Hf-in-zircon analyses from the Northwest Altaishan (n=107), Central Altai (n=164) and Qiongkuer-Abagong (n=311) terranes (see Table S6 in supplementary material). Cambrian to Carboniferous granitoids (ca. 507–313 Ma) show negative to positive zircon ε_{Hf} (t) values (Sun et al., 2008, 2009; Cai et al., 2010; Cai et al., 2011b,c; Yang et al., 2011; Cai et al., 2012a; Zhang et al., 2017a) and no difference in hafnium pattern according to the individual terranes (Fig. 10). At 400 Ma, the Hf-in-zircons switch from positive and negative values (-12 to +22) to only positive values ranging from +1 to +10 (Cai et al., 2011b,c; Zhang et al., 2017a). This may imply that both ancient and juvenile materials were involved in the magma before 400 Ma, but juvenile material prevailed in the magma source after 400 Ma (Sun et al., 2009). This switch in ε_{Hf} (t) values was attributed to the onset of ridge subduction and opening of slab window at ca. 420–400 Ma, resulted in massive supply of mantle melt (Sun et al., 2009; Jiang et al., 2010). Statistically, the Hf-in-zircon values for the granitoids are mostly positive, which can be interpreted as being due to a strong contribution of juvenile materials in the magma source. However, geochemical modelling shows that partial melting of the Habahe Group can produce the biotite-bearing granodiorites-granites and hornblende-bearing granodiorites-tonalites, which can have negative and positive epsilon Nd values if different proportions of components of this group were involved in the source (Jiang et al., 2016). This means that mantle derived juvenile materials could be less important than previously assumed (e.g. Wang et al., 2009a).

Figure 10 Hf isotopes granitoids about here

4. Metamorphism and its timing in the Chinese Altai

In this section we show that the Cambro-Devonian volcano-sedimentary sequences of the Chinese Altai are affected by three major tectono-metamorphic events. The peak mineral assemblages and peak P-T metamorphic estimation are presented in Table S7 of supplementary material and its metamorphic zonation is shown in the map of Figure 11. The review of existing quantitative pressure and temperature (P-T) are linked with different geotherms showing different tectonic settings for the three metamorphic events (Fig. 12). U–Pb zircon, monazite and $^{40}Ar/^{39}Ar$ ages provide chronological constraints on metamorphism and cooling of these distinct orogenic events (Figs. 11 and 13 and Table S8 in supplementary material).

4.1. Correlation between metamorphic zonation and boundaries of terranes

The metamorphic evolution of the Chinese Altai is characterized by three main thermal events; the first one is characterized by the Barrovian field gradient whilst the two last metamorphic events are Buchan type. The metamorphic zonation map shows that the Barrovian zones are marked by occurrence of kyanite, staurolite and garnet index minerals, while the Buchan zones are characterized by sillimanite, garnet and cordierite (Fig. 11). The Barrovian metamorphic assemblages are overprinted by LP metamorphic mineral assemblages (cordierite, andalusite) producing complex metamorphic associations and field isograd pattern (Zhuang, 1994; Wei et al., 2007; Jiang et al., 2015). The metamorphic map also shows that the metamorphic grade decreases towards the north-northwest, i.e. the North Altaishan and Northwest Altaishan terranes (Fig. 11), which are composed of the chlorite or biotite zones. In contrast, the Central Altai and Qiongkuer-Abagong terranes reached the maximum intensity of Barrovian metamorphism in wide kyanite–staurolite and garnet–staurolite zones and

migmatization. In addition, garnet–cordierite, K-feldspar–sillimanite and andalusite-bearing mineral assemblages in the Qiongkuer-Abagong terrane indicate an important Buchan type metamorphic re-equilibration. The LP-HT to UHT-HT metamorphism is also associated with an extensive development of various types of migmatites. Going further south, the metamorphic grade decreases and reaches biotite metamorphic zone in the South Altaishan terrane. Hence, the metamorphic map clearly shows that the metamorphic zonation correlates with the boundaries of some terranes that differ in metamorphic grade and also in sequence of metamorphic events (Figs. 11).

Figure 11 metamorphic map about here

4.2. P-T conditions and metamorphic ages of the three main metamorphic events

The first Barrovian metamorphic event occurred at P-T conditions ranging from 4–5 kbar at 550°C to 7–9 kbar at 650°C (Jiang et al., 2015). In detail, staurolite–garnet-bearing samples yielded conditions of 6.5 kbar at 540°C (Zhuang, 1994), while for other staurolite–garnet and kyanite–garnet-bearing schists conditions of 8 kbar at 580–600 °C were calculated in the Qiongkuer-Abagong terrane (see Table S7; Zhang et al., 2007). Some kyanite-bearing micaschists show prograde evolution from 6 kbar at 615°C to 8.7 kbar at 630°C (Wei et al. 2007). The Barrovian event is characterized by standard field metamorphic geotherm ranging from 20 to 25ºC/km typical for moderate mantle heat flow (e.g. Thompson et al., 2001) (Fig. 12a). So far, the Barrovian metamorphism was not dated in the Chinese Altai although Silurian to Early Devonian ages have been envisaged in the Mongolian Altai by some authors (Burenjargal et al., 2014).

Figure 12 PT diagram about here

The LP-HT Buchan-type event is characterized by the presence of sillimanite–cordierite-bearing migmatites, which gave P-T estimation of 8 kbar and 780°C (samples from the Qiongkuer-Abagong terrane, Jiang et al., 2015). In the same terrane, 6.4 kbar at 740°C were estimated for garnet–cordierite-bearing paragneiss (Zhang et al., 2007) and 6–7 kbar at 680°C to 3–4 kbar at 550°C for sillimanite–andalusite-bearing schists (Wei et al., 2007). The LP-HT metamorphism is characterized by rather hot metamorphic field geotherms ranging from 25 to 35ºC/km indicating elevated mantle heat flow typical for lithospheric thinning (e.g. Thompson et al., 2001) (Fig. 12b). The timing of this metamorphic event was constrained by U–Pb Devonian ages on zircon rims for the sillimanite–garnet-bearing paragneisses in the Northwest Altaishan, Qiongkuer-Abagong and South Altaishan terranes (ca. 384–390 Ma; Long et al., 2007; Jiang et al., 2010; Zhang et al., 2012; Li et al., 2014) and on U–Th–Pb monazite for metasediments in the South-East of the Central Altai terrane (ca. 377–381 Ma; Zheng et al., 2007). Altogether, the above isotopic results cover a large area and show that the Middle to Late Devonian metamorphism was extensive in the entire high-grade core of the Chinese Altai (see Fig. 11 and Table S8).

The last UHT-HT Buchan-type metamorphic event is restricted to a narrow zone along the southern margin of the Central Altai, Qiongkuer-Abagong and South Altaishan terranes (Fig. 11). Li et al. (2010) obtained a clockwise P-T path based on geo-thermobarometry from an UHT garnet–spinel–orthopyroxene-bearing granulite with peak conditions of 7 to 9.8 kbar at 960°C (see Table S7). Tong et al. (2014a) calculated a P-T path from a UHT garnet–spinel–orthopyroxene–sillimanite–cordierite–biotite-bearing granulite from 7 kbar at 890°C and 9 kbar at 970°C followed by re-equilibration at 8–9 kbar and 870°C. Li et al. (2014) calculated a (U)HT garnet–spinel–orthopyroxene–sillimanite–cordierite–biotite–K-feldspar-bearing granulite. In

addition, Wang et al. (2009b, 2014a) calculated for a pelitic garnet–cordierite–sillimanite–K-feldspar–biotite granulite P-T conditions of 5–6 kbar at 780–800°C and for sillimanite-bearing schist 5.6–6.8 kbar and 635–670°C, respectively. The UHT-HT event is characterized by exceptionally hot metamorphic field geotherms ranging from 30 to 40ºC/km that reflect elevation of mantle isotherms or massive intrusion of large volumes of hot magmas (e.g. Thompson et al., 2001) (Fig. 12c). The timing of this hot event is determined by the U–Pb dating of zircon rims and by the dating of metamorphic monazites (Fig. 11 and Table S8). In the Qiongkuer-Abagong terrane, zircon from a cordierite-bearing leucosome yielded an age of 300.8 ± 1.9 Ma (Broussolle et al., 2018), zircon rims from a sillimanite-bearing paragneiss yielded 299.2 ± 3.4 Ma (Wang et al., 2014b) and other zircon ages between 278 and 295 Ma were obtained from cordierite–orthopyroxene–garnet–spinel-bearing granulites (Wang et al., 2009b; Tong et al., 2014a). Permian monazite ages of ca. 261–268 Ma were obtained from schists of the Central Altai and Qiongkuer-Abagong terranes (Zheng et al., 2007). A range of radiometric ages were recorded in the South Altaishan terrane, where a zircon rim from a mica-schist was dated at 295.7 ± 3 Ma (Li et al., 2015a), zircon rims from a UHT granulite yielded ages between ca. 277 to 280 Ma (Li et al., 2014) and zircon crystallization age in a migmatite was determined at 283 ± 4 Ma (Zhang et al., 2012). Monazites from a garnet-bearing amphibolite and a metapelite schist of the South Altaishan terrane yielded 278 ± 9 Ma and 246 ± 18 Ma U–Pb ages, respectively (Briggs et al., 2007, 2009).

The zircon and monazite ages are plotted in probability density diagrams, which show that the Devonian metamorphic event is recorded in the whole Chinese Altai (Fig. 11). In the Northwest Altaishan terrane, the Devonian event seems to be dominant in comparison with the Central Altai, Qiongkuer-Abagong and South Altaishan terranes, where the Permian metamorphic event

is dominant (Fig. 11). Both Devonian and Permian zircon and monazite metamorphic ages are recorded in the high-grade core of the orogen, irrespective of terrane boundaries. The presence of both Devonian and Permian zircon rims indicates very high-grade metamorphism during both events that allowed the crystallization of zircon from melt during the regional anatexis (Jiang et al., 2010; Li et al., 2014; Tong et al., 2014a; Wang et al., 2014b; Broussolle et al., 2018).

4.3. Review of Chinese Altai $^{40}Ar/^{39}Ar$ ages

The $^{40}Ar/^{39}Ar$ ages in the Chinese Altai are spanning from Permian to Cretaceous (see Table S8; Laurent-Charvet et al., 2003; Yan et al., 2004; Briggs et al., 2007; Yuan et al., 2007; Briggs et al., 2009; Li et al., 2015b, 2017). The Permian to Triassic ages from the Qiongkuer-Abagong and South Altaishan terranes were interpreted either as a result of uplift and/or cooling of the Chinese Altai (Li et al., 2015b). For example, shearing may reset the argon system along thrust faults (Briggs et al., 2009), and $^{40}Ar/^{39}Ar$ ages were interpreted to record strike slip motion of the Erqis shear zone in the South Altaishan terrane (Laurent-Charvet et al., 2003; Yan et al., 2004; Briggs et al., 2007; Li et al., 2015a). Li et al. (2017) interpret these $^{40}Ar/^{39}Ar$ ages to record cooling after amphibole-facies metamorphism in the Erqis shear zone. Therefore, the available U–Pb geochronological data provide enough evidence that the whole Chinese Altai underwent the same succession of metamorphic events, irrespective of terrane boundaries. Nevertheless, the Triassic to Jurassic ages in the Central Altai and Qiongkuer-Abagong terranes were interpreted as reset ages due to the thrust faults (Briggs et al., 2009) or the intrusion of the Keketuohai batholith in the Triassic (Wang et al., 2014a).

Figure 13 $^{40}Ar/^{39}Ar$ about here

5. Tectono-metamorphic history of the Chinese Altai

Here, we present the metamorphic evolution of the Chinese Altai together with a review of the polyphase deformation. An attempt is made to correlate the orogenic fabrics with the metamorphic events and its timing in the frame of the geodynamic evolution of the Chinese Altai (see Fig. 14).

According to previous structural studies carried out in the Chinese Altai (Qu and Zhang, 1994; Wei et al., 2007; Li et al., 2015a; Jiang et al., 2015; Zhang et al., 2015; Li et al., 2016b; Broussolle et al., 2018), several deformation events affecting the Cambrian to Devonian rocks can be distinguished. Although these authors do not agree on the number of phases, almost all of them describe an early main metamorphic foliation affected by upright folding. According to Zhang et al. (2015), the western part of the Chinese Altai is affected by a penetrative and sub-horizontal S1 foliation related to a NW-SE directed D1 shortening. Subsequently, the metamorphic fabric was reworked by a NE-SW directed shortening deformational D2 event, characterized by a NW-SE trending subvertical S2 cleavage. Similar observations were made by Jiang et al. (2015) in the nearby section of the western Chinese Altai, where a sub-horizontal metamorphic fabric was reworked by large scale NW-SE trending upright folds. In contrast, Broussole et al. (2018) and Jiang et al. (in review) clearly showed that in the central and eastern parts of the Chinese Altai the early metamorphic sub-horizontal fabric was reworked by two phases of mutually orthogonal upright folds. The first upright folding event resulted in the formation of NE-SW trending gneiss domes cored by migmatites and granites that were refolded by NE-SW trending upright folds and heterogeneous NE-SW striking cleavage zones. Consequently, the structural sequence in the NW part of the Chinese Altai described by Zhang et al. (2015) and Jiang et al. (2015) can be regarded as a result of two-phases Devonian

metamorphism and deformation rotated to NE-SW direction by a large scale Permian oroclinal bend. The large scale bending can also explain the lack of a Permian cleavage in this area, which displays only NE-SW trending limb of megafold.

5.1. Early Paleozoic metamorphism and D1 deformation

The metamorphic zonation map shows that the Barrovian metamorphism affected the entire mountain range (Fig. 11). This metamorphism was associated with the development of a regional schistosity S1 that was originally sub-horizontal and characterized by a syn-schistose growth of biotite, garnet, staurolite and kyanite in the Qiongkuer-Abagong and the Central Altai terranes (Wei et al., 2007; Jiang et al., 2015; Zhang et al., 2015, Li et al., 2016b; Broussolle et al., 2018). In the western part of the Qiongkuer-Abagong terrane, the kyanite, staurolite and garnet crystals with inclusion trails interpreted as S1 are preserved in sillimanite-bearing migmatites (Jiang et al., 2015). Although no metamorphic age was published so far from Barrovian schists, several authors suggested that the D1 deformation occurred prior to the Late Devonian because the S1 schistosity is folded by the Late Devonian-Early Carboniferous upright F2 folds and in some places is transposed by the S2 foliation (Fig 14; Jiang et al., 2015; Zhang et al., 2015; Broussolle et al., 2018; Jiang et al., in review). Unfolding of Late Devonian to Early Carboniferous F2 upright folds clearly point out to a sub-horizontal attitude of S1 fabric (Zhang et al., 2015; Broussolle et al., 2018).

However, there are several studies from the Chinese and Mongolian Altai which showed that the deep crust was affected by the partial melting and the development of LP-HT mineral assemblage. The migmatization is related also to the development of a sub-horizontal foliation and extensional shear bands pointing to an important vertical shortening of the Altai accretionary wedge at this time (Hanžl et al., 2016; Broussole et al., 2018; Jiang et al., in review). Altogether,

the attitude of the Barrovian metamorphic foliation, the LP-HT migmatititic and associated granitic fabrics were both sub-horizontal but in some places the migmatites contain relics of Barrovian minerals such as kyanite and staurolite (Jiang et al., 2015). Therefore, it is proposed that the earliest Barrovian fabric was related to crustal thickening, while the intrusion of granite sheets and melting of deep crust were related to large scale crustal extension, consistent with addition of volcano-sedimentary sequence during the LP-HT Devonian metamorphism. In this model, the two events produced fabric of the same sub-horizontal geometry, but the extension and associate anatexis is younger than the Barrovian event. Keeping in mind the parallelism of the two fabrics, Jiang et al., (in review) used $D1_B$ index for the Barrovian fabric and $D1_M$ for the later extensional migmatitic foliation, which is also adopted in this paper (see Fig. 14).

5.2 Late Devonian-Early Carboniferous upright F2 folding and crustal scale doming

D2 deformation is Late Devonian-Early Carboniferous in age and is expressed by the development of upright F2 folds associated with the heterogeneously developed sub-vertical S2 fabric (Zhang et al., 2015; Broussolle et al., 2018). In the Qiongkuer-Abagong terrane, the NW-SE trending S2 fabric transposes the S1 fabric in sillimanite–garnet-bearing migmatites and highly foliated granitoids (Jiang et al., 2015). In contrast, structural study of Zhang et al. (2015) in the northern part of the Qiongkuer-Abagong terrane shows that this D2 event is characterized by a NE-SW trending sub-vertical foliation with no apparent metamorphism associated. These results are in agreement with structural investigations of Broussolle et al. (2018) and Jiang et al., (in review) in the central part of the Qiongkuer-Abagong terrane, where the S1 schistosity was rotated by a NE-SW trending upright F2 fold in fold limbs (Fig 14). These two structural studies show that the D2 event occurred under NW-SE compressive regime and in some places formed a new NE-SW trending sub-vertical S2 fabric related to the major crustal scale doming event.

Devonian amphibolite-facies peak assemblages are developed in hinge zones of these antiformal structures and are related to the exhumation of the partially molten lower crust (Jiang et al., 2015). Similar process was reported in Mongolia where the crustal-scale folding is associated with the exhumation of hot granitoids and migmatites in the core of kilometer scale antiforms (Broussolle et al., 2015; Lehmann et al., 2017).

Figure 14 Deformation in the Chinese Altai

5.3. Permian metamorphism and D3 deformation

D3 deformation is expressed by large bend thrust systems or oroclines (Qu and Zhang, 1994). Their kinematic data suggest that the rocks forming the core of the Altai were thrust obliquely from the northeast to the southwest. Recent geochronological studies show that these oblique thrust systems can be dated at Late Permian to Triassic (e.g. Laurent-Charvet et al., 2003; Yan et al., 2004; Briggs et al., 2007; Yuan et al., 2007; Briggs et al., 2009; Li et al., 2015b, 2017). In addition, several authors observed a greenschist-facies penetrative schistosity associated with a NW-SE upright D3 folding in the whole Qiongkuer-Abagong and South Altaishan terranes (Li et al., 2015a; Zhang et al., 2015; Broussolle et al., 2018). These observations are consistent with the study of Broussolle et al. (2018) for the central part of the Qiongkuer-Abagong terrane where the D3 deformation is associated with cordierite–sillimanite–garnet-bearing migmatites that were exhumed along a tabular NW-SE trending zone of several kilometers wide and tens kilometers long. This zone is characterized by the development of a penetrative and high-grade schistosity geometrically coherent with greenschist facies D3 fabrics elsewhere. The Permian age of these high-grade rocks is confirmed by zircon rim U–Pb ages ranging from ca. 300 to 270 Ma (Fig. 14; Wang et al., 2009b; Cai et al., 2011c; Tong et al., 2013, 2014a; Wang et al., 2014b; Broussolle et al., 2018). Broussolle et al. (2018) and Jiang et al. (in review) also showed that the Permian

amphibolite- to granulite-facies D3 deformation reworked all previous Devonian structures and mineral fabrics. Based on geometrical coherence and radiogenic dating, it was proposed that the age of the D3 deformation ranges between ca. 322 and 252 Ma (Li et al., 2015a) but recent datings of Broussolle et al. (2018) and Jiang et al. (in review) indicate that the main Permian shortening operated between 300 and 270 Ma, with the main peak around 280 Ma. All these studies show that the major D3 deformation was mainly localized in the southern part of the Chinese Altai and intensively affected the Qiongkuer-Abagong and South Altaishan terranes (see Fig. 11). In addition, this major NW-SE trending F3 folding phase was also observed and described at the margin of the Central Altai and the South Qiongkuer-Abagong terranes by Qu & Zhang (1994), indicating that this D3 event could be extended until the southern part of the Central Altai terrane.

During the last Permian event (D3) migmatites and granulites were formed and exhumed along the margin of the Qiongkuer-Abagong and South Altaishan terranes. Even if some authors assumed that the origin of UHT-HT metamorphism was associated with the activity of the Tarim mantle plume at ca. 280 Ma (Li et al., 2014; Tong et al., 2014a), the time span of ca. 300–270 Ma of the Permian high-grade event and the recent structural studies suggest that a compressive setting was responsible for the exhumation of these rocks (Broussolle et al., 2018). Therefore, the Early Permian event is attributed to collision of the Chinese Altai orogenic belt and the Junggar arc system while the Late Permian to Triassic deformation is attributed to continuous strike slip movements along the Erqis shear zone (Briggs et al., 2007; Li et al., 2015a; Zhang et al., 2015).

In conclusion, the Middle Paleozoic event affected all the five terranes while the UHT-HT Permian event seems to affect only narrow NW-SE zone along the Qiongkuer-Abagong and South Altaishan terranes (Fig. 11). The Silurian to Early Devonian $D1_B$ event corresponds to a

moderate crustal thickening accommodated by sub-horizontal crustal flow, while the mid-Devonian $D1_M$ event was related to large scale crustal extension and partial melting of the Altai wedge associated with intrusions of granite sheets in the middle and upper crust. In contrast, the Late Devonian D2 event developed under a NW-SE compressive regime and resulted to the crustal scale doming. Finally, the Permian D3 event occurred under NE-SW compressive regime and is characterized by ubiquitous upright folding, thrusting, bending and development of NW-SE oriented deformation zones (Qu and Zhang, 1994; Briggs et al., 2007). The D3 intensity is maximal in the southern part of the Chinese Altai (Li et al., 2015a; Zhang et al., 2015; Broussolle et al., 2018), where it reworked and transposed all the previously developed orogenic fabrics. Finally, the tectono-metamorphic zones resulting from the three metamorphic events are highlighted in the Chinese Altai map and broadly correspond to the terranes proposed by Windley et al. (2002) (Fig. 14).

6. Discussion

6.1. Lack of Precambrian basement in the Chinese Altai

The possible existence of a Precambrian basement in the Chinese Altai (Windley et al., 2002; Wilhem et al., 2012) has been discussed by numerous authors. A model of an old microcontinent covered by Early Paleozoic passive margin sequences was proposed (Wang et al., 2009a; Yang et al., 2011; Zhang et al., 2017b). However, recent isotopic studies show that the Chinese Altai was an active margin in the Paleozoic (Long et al., 2007; Sun et al., 2008) mainly composed of volcano-sedimentary material of an accretionary wedge intruded by granitoids (Jiang et al., 2016, 2017). The paragneisses were considered to represent a Precambrian basement of the Chinese Altai, but a small number of detrital zircons have been dated and the results support that the accretionary wedge was mainly composed of a Cambro-Ordovician turbiditic sequence with

detritus dominantly 438 and 528 Ma old (see Table S1; Long et al., 2007; Sun et al., 2008; Long et al., 2010; Jiang et al., 2010, 2011; Yang et al., 2011; Wang et al., 2014c; Zhang et al., 2015; Broussolle et al., 2018). In addition, zircon Hf isotope results show that the Paleozoic granitoids came from a juvenile source, instead of a Precambrian lower crust (Long et al., 2007; Sun et al., 2008, 2009; Cai et al., 2010, 2011a,b,c; Yang et al., 2011; Cai et al., 2012a; Zhang et al., 2017a). Some Precambrian detrital zircons occur in the Paleozoic sedimentary rocks, because of the lack of ancient rocks in the Chinese Altai, these old grains are interpreted as exotic detritus transported from the eroded Precambrian Mongolian microcontinental blocks (Jiang et al., 2011). A small number of inherited zircons are found in gneissic granites and migmatites which can be interpreted to be captured from an assumed Precambrian basement (Zhang et al., 2017b). However, these inherited zircons are indistinguishable, in term of age and Hf isotopic signature, from the exotic old detrital zircons in the Paleozoic metasediments. Therefore, these inherited zircons could be xenocrysts from the metasediments (Jiang al., 2016). The above discussion indicates that there is no concrete evidence to support the existence of a Precambrian basement in the Chinese Altai and more likely the whole domain represents a Paleozoic accretionary wedge bordering the Mongolian microcontinental blocks further north (Long et al., 2007; Sun et al., 2008; Cai et al., 2010; Jiang et al., 2016, 2017).

However, Kruk et al., (2018) proposed an alternative explanation suggesting that the sediments are not developed in accretionary – subduction setting but merely as a result of interplay between plate tectonic and plume activity processes. These conclusions are at odds with the cumulative distribution curves of detrital zircon spectra from the Chinese, Mongolian and Russian Altai (Fig. 15). This plot shows that all the detrital zircon data from the Altai Mountains in China, Russia and Mongolia are consistent with active margin setting.

6.2. Interpretation of the tectono-metamorphic evolution of the Chinese Altai

The first tectono-metamorphic event recorded in the Chinese Altai is the Barrovian prograde metamorphism associated with sub-horizontal schistosity $S1_B$ (Wei et al., 2007; Jiang et al., 2015; Zhang et al., 2015, Li et al., 2016b; Broussolle et al., 2018; Jiang et al., in review). This event is interpreted to result from moderate thickening of the Altai accretionary wedge (Fig. 14; Jiang et al., 2015). The $S1_B$ fabric was subsequently exploited by sheet like intrusions of granitoids that were gneissified at ca. 400–380 Ma. During this period, sillimanite grew in sub-horizontal migmatitic $S1_M$ fabric, as it was observed in the Chinese Altai by Broussolle et al. (2018) and Jiang et al. (in review) or in the Mongolian Altai by Hanžl et al. (2016). This new mineral assemblages was associated with a deep crustal melting that can be interpreted to result from a large scale heat input from the mantle, or a decompression associated with an exhumation of highly radiogenic rocks during the crustal-scale extension and/or the vertical shortening of a hot wedge (Zhang et al., 2015; Hanžl et al., 2016; Broussole et al., 2018; Jiang et al., in review). The latter interpretation is supported by: 1) the presence of numerous gneissified granite to tonalite sub-horizontal sills reactivating the S1 anisotropy (e.g. Hanžl et al., 2016; Broussolle et al., 2018), and 2) the sedimentation of Devonian detrital sediments in the Kangbutiebao and Altai formations that were deposited between ca. 407 and 382 Ma. In particular, the Kangbutiebao and Altai formations are characterized by a thick sequence of sedimentary and turbiditic rocks, and by basaltic volcanic rocks that were interpreted both in China as an onset of extensional tectonics (Zhang et al., 2015; Broussolle et al., 2018; Jiang et al., in rewiew). Exactly the same conclusion can be made for the Mongolian equivalent of the Chinese Altai Devonian sequences (Demoux et al., 2009; Lehmann et al., 2010). Recent work of Soejono et al. (2018) brings strong sedimentary and geochronological arguments supporting the Devonian extensional

reworking of the Altai orogenic edifice. The sub-horizontal schistosity $S1_M$ and sheets of granitoids were subsequently folded by upright F2 folds during NW-SE compression that was associated with extrusion of granitoids in cores of the gneiss domes (Fig. 14; Jiang et al., 2015; Zhang et al., 2015; Broussolle et al., 2018). The D2 event is characterized by the exhumation of sillimanite–cordierite-bearing migmatites in cores of giant dome structures (Jiang et al., 2015). This event was dated in the Mongolian Altai as Late Devonian – Early Carboniferous by U–Pb method on zircons and monazites (Broussolle et al., 2015; Nakano et al., 2015; Lehmann et al., 2017) and was possibly also recorded in the Chinese Altai by 360 Ma metamorphic overgrowths of magmatic (Cai et al., 2011c) and detrital zircons (Li et al., 2014). Finally, the Permian NE-SW compression occurred during ca. 300 to 250 Ma in the whole CAOB and is well expressed by giant NW-SE trending deformation fronts in the whole Altai (Fig. 14; Edel et al., 2014; Guy et al., 2014a,b; Li et al., 2015a; Broussolle et al., 2018). In the studied region, the Permian shortening is a response of collision between the Junggar arc system and the Chinese Altai orogenic belt both squeezed between the North China-Tarim and Siberian cratonic jaws (Lehmann et al., 2010; Xiao et al., 2015).

6.3. Absence of *'terranes'* in the Chinese Altai

Terranes should be in theory units with different lithostratigraphy content and contrasting tectonic evolution limited by distinct vertical deformation zones like strike slips, transform faults or sutures (Coney et al., 1980; Sengör and Dewey, 1990). In the Chinese Altai, the different stratigraphic units have been defined and limited by faults with supposed large-scale displacement (see Fig. 1; Windley et al., 2002; Xiao et al., 2004). However, studies of variously metamorphosed turbiditic sediments show that the principal Cambro-Ordovician Habahe Group is present in the whole Chinese Altai as the main lithology irrespective of "terrane" boundaries

(Long et al., 2007; Sun et al., 2008; Jiang et al., 2011; Wang et al., 2014c; Broussolle et al., 2018). The U–Pb detrital zircon age pattern depicted in the four terranes forming the Chinese Altai is coherent with an active margin setting (Cawood et al., 2012) and shows that the significant proportion of zircon ages is close to the depositional age of the sediments. Therefore, the stratigraphy (Fig. 4), zircon age spectra (Fig. 5) and Hf-in-zircon pattern (Fig. 6) suggest that the Chinese Altai can be considered as a giant accretionary wedge composed of detritus from the giant Cambro-Ordovician magmatic arc (Ikh-Mongol arc of Janoušek et al., 2018), Proterozoic arc rocks of the Lake zone and the eroded basement of the Mongolian microcontinental blocks to the north (Jiang et al., 2011, 2016, 2017). This Cambro-Ordovician accretionary wedge was subsequently unconformably covered by two volcano-sedimentary Kangbutiebao and turbiditic Altai formations of Lower to Middle Devonian ages, respectively (Chai et al., 2009; Broussolle et al., 2018) and by the Carboniferous Kalaerqisi volcano-sedimentary sequence (Chen and Jahn, 2002; Li et al., 2015a, 2017). The deposition of the Devonian sedimentary formations coincides with the climax of the emplacement of Devonian granitoids in the crust (Fig. 7) and represents a general event affecting the bulk of Altai wedge. In contrast, the regional distribution of Carboniferous cover can be regarded as a result of erosion of uplifted high-grade core of the Chinese Altai probably during the D2 folding and doming (Fig 14; e.g. Lehmann et al., 2010). Looking from this perspective, the preservation of low-grade Paleozoic sediments in the north and south does not necessarily imply presence of terranes with distinct stratigraphic and tectonic evolution.

However, the Kalaerqisi complex was interpreted to be a Paleozoic accretionary wedge complex based on the lithology composed of off-scraping materials and continent-sourced sediments (Briggs et al., 2007, 2009; Xiao et al., 2009). If this is a case, at least Carboniferous

sequences of the South Altai terrane can represent lateral accretion of distinct lithological unit – a true terrane, along the southern Chinese Altai, rather than its sedimentary cover.

Studies of the Cambrian to Carboniferous granitoids have shown that they intruded the whole area irrespective of the terrane boundaries (Yuan et al., 2007; Wang et al., 2009a; Cai et al., 2011c; Cai et al., 2012a; Yu et al., 2017; Zhang et al., 2017a). These syn-subduction and mainly Devonian granitoids are geochemically identical (Fig. 8), show mostly juvenile signature (Figs. 9 and 10) and originated through melting of the Cambro-Ordovician accretionary wedge (Jiang et al., 2016). Permian granitoids are all characterized as a post-subduction orogen (Tong et al., 2014b and references therein) and occur close to the Erqis suture zone (Fig. 7). Altogether, the presence of Devonian granitoids over the Chinese Altai clearly invalidates the terrane hypothesis, as they indicate one giant anatectic process, which unevenly affects the whole Chinese Altai. The limitation of Permian granitoids in the south results of a major thermal perturbation at the Junggar arc system and the Chinese Altai boundary but has no "terranological" significance.

Structural and metamorphic studies show that the Early to Middle Paleozoic Barrovian and Buchan events extensively affected large parts of the Chinese Altai (Fig. 11) irrespective of terrane boundaries with exception of limits between low-grade rocks in the north and high-grade rocks in the central part of the Chinese Altai (Fig. 15). In addition, the Permian UHT-HT Buchan-type event is located along wide NW-SE zone covering the Qiongkuer-Abagong and South Altaishan terranes (Figs. 11 and 15). The distribution of polycyclic metamorphism thus marks different terranes boundaries even if regional distribution of various U–Pb zircon and monazite metamorphic and $^{40}Ar/^{39}Ar$ cooling ages shows that the whole Chinese Altai was affected, albeit heterogeneously, by the same sequence of tectono-metamorphic events. The

"terranes" marked by distinct greenschist, amphibolite or even granulite-facies metamorphism thus represent only different levels of the same orogenic crust with the Cambro-Ordovician protolith (Jiang et al., 2015; Broussolle et al., 2018), which we call here "orogenic domains". This is particularly valid for greenschist facies orogenic domain forming the northern and north-western parts of the Chinese Altai (North Altaishan and Northwest Altaishan terranes). This region is not considered as an assemblage of distinct terranes here, but as an orogenic domain, where accretionary wedge was affected by low-grade Devonian metamorphism only (Fig. 16). Similarly, the Central Altai and Qiongkuer-Abagong terranes cannot be interpreted as distinct terranes but as a specific orogenic domain where highly metamorphosed and partially molten Devonian orogenic lower crust was exhumed to supracrustal levels. This orogenic domain thus represents a high grade metamorphic core of the Chinese Altai that was tectonically juxtaposed to the low-grade supra-crustal orogenic domain in the west and north during Devonian orogeny (Fig. 16). Likewise in the north, the southern Qiongkuer-Abagong and South Altaishan terranes are newly interpreted here as a 50 Km wide and several hundred kilometres long NW-SE trending orogenic domain where Devonian orogenic lower, middle and upper crust was heterogeneously reworked by Permian metamorphism, deformation and magmatism. This orogenic domain represents a collisional zone between Junggar arc and Altai orogenic belt and reflects a region of most important interference between Devonian and Permian orogenic fabrics (Fig. 15). In conclusion, instead of "terranes" we propose here a simplified sub-division of the Chinese Altai wedge into the upper crustal and lower-grade Devonian orogenic domain in the north (NW Altaishan and N Altaishan terranes), the lower crustal Devonian orogenic domain in the centre (high-grade core of the mountains corresponding to the central Altai terrane) and the

high-grade Permian orogenic domain in the south (Qiuongkuer-Abagong and South Altaishan terranes).

Figure 16 tectono-metamorphic map of Chinese Altai

The bulk of the Chinese Altai orogenic structure was already formed during the $D1_{B-M}$ event, when a vertically stratified crust originated, marked by a sub-horizontal orogenic fabric, sheets of granitoid sills, the $M1_{B-M}$ metamorphic grade increasing with depth and the deposition of sediments at the surface. The $M1_{M}$ metamorphic zones of the Chinese Altai were subsequently perturbed by the Late Devonian to Early Carboniferous upright F2 folding and the development of the mantled gneiss domes cored by granitoids. Both the upright F2 folds and gneiss domes were trending originally NE-SW thereby providing first alternations of high- and low-grade domains, separated by vertical zones of deformation. Subsequently, the whole system was affected by the giant NE-SW shortening event that culminated by the NW-SE trending upright F3 re-folding of both the upright F2 folds and elongated gneiss domes and the transposition of all the previous structures by steep NW-SE trending D3 deformation zones. The large-scale vertical tabular zone of Permian granulites in the south thus represents the most pronounced expression of this giant Permian D3 event. The complexity of "terrane" distribution of the Chinese Altai is a result of many factors, but namely the superposition of two horizontal shortening events, that generated variably exhumed originally horizontally disposed crustal levels separated by vertical boundaries. The lack of differences between the individual terranes of the Chinese Altai matches very well with the gravity map (Fig. 3) that does not reveal any gradient parallel to the "terrane" boundaries. In fact, the gravity signal confirms lithological and tectonic homogeneity of the Chinese Altai.

Overall, stratigraphy, magmatism, metamorphism, deformation and geophysical patterns show that the Chinese Altai is not composed of different terranes accreted altogether but represents a coherent domain defined as a huge accretionary wedge, which is extending from Russia to Mongolia (Jiang et al., 2017). This giant accretionary wedge rims the giant and long living magmatic arc developed on the Mongolian ribbon continent during Early Paleozoic (Şengör et al., 1993; Jiang et al., 2017; Janoušek et al., 2018).

6.4. Paleozoic evolution of the CAOB

The Paleozoic evolution of the Chinese Altai is governed by the long lasting, Cambrian to Late Ordovician activity of the Ikh-Mongol arc system that evolved above the oceanic subduction dipping to north, beneath the Mongolian ribbon continent (Buriánek et al., 2017; Janoušek et al., 2018). After the termination of the Ikh Mongol arc activity the accretionary wedge was reworked by Late Ordovician to Devonian magmatism that is possibly related to continuous roll back of the subducting slab (Jiang et al., 2016). The deep part of the Altai accretionary prism was molten and partly transformed to LP-HT granulites at around 400–380 Ma (Jiang et al., 2010, 2012; Burenjargal et al., 2014; Broussolle et al., 2015; Nakano et al., 2015). This LP-HT metamorphism was preceded by a MP-MT burial event during possibly short-lived moderate thickening of the whole wedge. The potential closure of remnants of the oceanic domain occurred between the Altai accretionary wedge and the Junggar arc system along the Erqis shear zone (Li et al., 2015a, 2017). The collision occurred between ca. 300 and 280 Ma as manifested by several features: 1) an extinction of syn-subduction magmatism in the Chinese Altai at ca. 313 Ma (Yuan et al., 2007; Cai et al., 2012a); 2) the activity of the Erqis shear zone from ca. 290 to 250 Ma (Laurent-Charvet et al., 2002; Buslov et al., 2004; Li et al., 2015a, 2017); 3) the Permian crustal scale folding and exhumation of granulites and migmatites in the

southern part of the Chinese Altai from ca. 300 to 280 M (Li et al., 2014; Tong et al., 2014a; Broussolle et al., 2018); and finally, 4) the post-subduction magmatism in the Chinese Altai from ca. 280 to 250 Ma (Tong et al., 2014b and references therein). A compressional activity still continued between ca. 280 to 240 Ma in the Chinese Altai as exemplified by transpressional movements along the Erqis shear zone (Li et al., 2015a, 2016a).

7. Conclusions

- The main sedimentary sequence forming the Chinese Altai is the Cambro-Ordovician Habahe Group that is present in the Northwest Altaishan, Central Altai, Qiongkuer-Abagong and South Altaishan terranes and potentially also in the North Altaishan terrane. This flyshoid sequence extends as 1500 km long belt from the Russian to Mongolian Altai.
- Distribution, geochemistry and isotope features of syn-subduction granitoids show that they can be regarded as a single group of granitoids, similar to those intruding the Tugrug (Habahe) Group in Russian and Mongolian Altai.
- There are three types of deformation and metamorphism in the Chinese Altai: the first MP-MT Barrovian metamorphism formed during moderate thickening, followed by the LP-HT Buchan type metamorphism related to intrusions of syn-subduction granitoids during an extensional setting and subsequently, affected by the NW-SE Late Devonian – Early Carboniferous shortening. Finally, the Permian collision between the Chinese Altai orogenic belt and the Junggar arc system provoked a NE-SW shortening event resulting in a crustal scale upright folding and an extrusion of UHT-HT granulites and migmatites.

- The supposed terranes are absent in the Chinese Altai. It can be regarded as a single Cambro-Ordovician accretionary complex reworked by widespread Devonian magmatism and metamorphism. Its southern part was further reworked by the Permian granulite facies metamorphism. The supposed "terranes" are not terranes in the sense how terranes are defined, but are domains formed by different crustal levels that are mutually juxtaposed during Devonian and Permian orthogonal shortening events.

Figure captions

Fig 1: Main tectonic map of the Central Asian Orogen Belt (CAOB; modified from Jiang et al. 2017). The Chinese Altai (the study area) is delineated by white contour and shown in Figure 2.

Fig 2: Generalized geological map of the Chinese Altai showing the different supposed terranes and boundaries/faults according to Windley et al. (2002) and Xiao et al. (2004) and the main lithostratigraphical units (modified after Li et al., 2015b).

Fig 3: Complete Bouguer gravity anomaly map of the Chinese Altai and adjacent regions (combined data provided by EGM08). The white lines and dashed lines represent the supposed boundaries/faults of the distinct terranes.

Fig 4: Synthetic stratigraphic column for the Paleozoic volcano-sedimentary sequences of the Chinese Altai including the intrusive sheets of different magmatic events and the timing of different metamorphic events. Stratigraphic data from BGMRX (1978) and Windley et al. (2002).

Fig 5: Geological map of the Chinese Altai showing the distribution of all available U–Pb detrital zircon ages (see geological legend in Figure 2). Relative probability density plots of detrital zircon grains in the range 0–3000 Ma are shown for 4 different terranes defined in the

Chinese Altai. Data with > 15% discordance are excluded. For comparison, the age distribution of the different grains is underlined by colours (see upper legend inset). For data and references, see Table S1 in the supplementary material.

Fig 6: ε_{Hf} (t) versus U–Pb ages diagram showing the results for detrital zircons available from 4 different terranes defined in the Chinese Altai. The colour-highlighted age intervals are defined by different types of ε_{Hf} (t) signature. See the Table S1 in supplementary material for all available Hf-in-zircon data.

Fig 7: Geological map of the Chinese Altai showing the distribution of all available U–Pb crystallization ages obtained for Paleozoic granitoids (see geological legend in Figure 2). Relative probability density plots of magmatic zircons are represented for 5 different terranes defined in the Chinese Altai. For comparison, the Devonian and Permian peaks are underlined (see upper legend inset). For data and references, see the Table S2 in supplementary material.

Fig 8: Geochemical characteristics of the Cambrian to Carboniferous granitoids from 4 different terranes defined in the Chinese Altai: a) Na_2O+K_2O versus SiO_2 diagram (after Cox et al., 1979), b) A/CNK $(Al_2O_3/CaO+Na_2O+K_2O)_{molar}$ versus A/NK $(Al_2O_3/Na_2O+K_2O)_{molar}$ (after Shand, 1943), c) K_2O versus SiO_2 diagram (after Peccerillo and Taylor, 1976), and d) (Na_2O+K_2O)-F_2O_3*5-((CaO+MgO)*5) ternary diagram (after Grebennikov et al., 2014). Diagrams are plotted by the GCD KIT package of Janoušek et al. (2006). For data and references see the Table S3 in supplementary material.

Fig 9: a) Whole-rock ε_{Hf}(t) versus U–Pb ages diagram for Devonian granitoids from 4 different terranes defined in the Chinese Altai. For data and references see the Table S4 in supplementary material. b) Whole-rock ε_{Nd}(t) versus U–Pb ages diagram for Cambrian to Carboniferous

granitoids from 4 different terranes defined in the Chinese Altai. For data and references see the Table S5 in supplementary.

Fig 10: ε_{Hf} (t) versus U–Pb ages diagram showing the results for magmatic zircons obtained from granitoids of 3 different terranes defined in the Chinese Altai. The vertical line at 400 Ma represents the change of Hf signature from negative to positive values (Sun et al., 2009), after 400 Ma ε_{Hf} (t) is only positive. For data and references see the Table S6 in supplementary material.

Fig 11: Metamorphic zoning map of the Chinese Altai showing the U–Pb metamorphic zircon and monazite ages, redrawn from Li et al. (2015b). Relative probability density plots of zircon and monazite ages are plotted for 4 different terranes defined in the Chinese Altai. For comparison, Devonian and Permian metamorphic events are colour-highlighted (see upper legend inset). For data and references see the Table S8 in supplementary material.

Fig 12: Geothermal gradients and published P-T paths for peak metamorphic assemblages of the three different Paleozoic metamorphic events: (a,b) Early to Middle Devonian P-T paths from Jiang et al. (2015, 2016), and (c) Early Permian P-T paths from Li et al. (2014), Tong et al. (2013, 2014a) and Wang et al., (2009b, 2014b). For data and references see the Table S7 in supplementary material. The thermal conditions limited by two geotherms of the different metamorphic events are colour-highlighted in pink, red and violet, corresponding to the colours of the different tectono-metamorphic domains used in the Figures 14 and 16.

Fig 13: Relative probability density plots showing the $^{40}Ar/^{39}Ar$ ages in the Chinese Altai according to three individual terranes. For comparison, the cooling phase is distinguished from

the transform and thrust faults highlighting them by two different colors. For data and references see the Table S8 in supplementary material.

Fig 14: Schematic diagram summarizing the timing of metamorphism, the deformational episodes and the possible tectonic setting (modified after Zhang et al., 2015 and Broussolle et al., 2018) in the Chinese Altai. Age constraints are also compiled in the Table S8 of supplementary material.

Fig. 15: (a) Cumulative accumulation curves of detrital zircon age spectra and (b) Cumulative distribution curves of differences between the crystallization ages (CA) and the depositional ages (DA) of the detrital zircons from the Chinese Altai (see references in the Table S1 of supplementary material), the Mongolian Altai (Jiang et al., 2017; Soejono et al., 2018) and the Russian Altai (Chen et al., 2015). Colour fields represent different tectonic setting of deposition (after Cawood et al., 2012).

Fig 16: Preliminary Chinese Altai map showing the different tectono-metamorphic orogenic domains. The North Altaishan and Northwest Altaishan correspond to the low-grade Devonian upper crust. The Central Altai terrane corresponds to the high-grade Devonian lower crust. The Qiongkuer-Abagong and South Altaishan terranes correspond to the high-grade Devonian metamorphic lower crust reworked by the Early Permian UHT-HT metamorphism.

Acknowledgement

This study was financially supported by the National Key Research and Development Program of China (2017YFC0601205), the NSF China (41672056, 41230207), the International Partnership Program of the Chinese Academy of Sciences (132744KYSB20160005), the Hong

Kong RGC research projects (17303415 and 17302317), the HKU grants (201411159173 and 201511159199), and by the Czech Science Foundation (GACR grant 17–17540S). The work forms part of the PhD thesis by A. Broussolle. A 100 Talents Program of the Chinese Academy of Sciences to JYD is also acknowledged. This is a contribution to IGCP 662. We thank editorial work of Prof. M. Santosh and two anonymous reviewers for their thoughtful and constructive reviews which greatly improved the paper.

References

Badarch, G., Cunningham, C.W. and Windley, B.F., 2002. A new terrane subdivision for Mongolia: implications for the Phanerozoic crustal growth of Central Asia. Journal of Asian Earth Sciences, 21(1): 87–110.

BGMRX, 1978. Geological Map of the Altai Sheet: Scale1: 200,000 (Unpublished).

Bold, U., Crowley, J.L., Smith, E.F., Sambuu, O. and Macdonald, F.A., 2016. Neoproterozoic to early Paleozoic tectonic evolution of the Zavkhan terrane of Mongolia: Implications for continental growth in the Central Asian belt. Lithosphere, 8(6): 729-750.

Briggs, S.M., Yin, A., Manning, C.E., Chen, Z.L. and Wang, X.F., 2009. Tectonic development of the southern Chinese Altai Range as determined by structural geology, thermobarometry, 40Ar/39Ar thermochronology, and Th/Pb ion-microprobe monazite geochronology. Geological Society of America Bulletin, 121(9-10): 1381-1393.

Briggs, S.M., Yin, A., Manning, C.E., Chen, Z.L., Wang, X.F. and Grove, M., 2007. Late Paleozoic tectonic history of the Ertix Fault in the Chinese Altai and its implications for the development of the Central Asian Orogenic System. Geological Society of America Bulletin, 119(7-8): 944-960.

Broussolle, A., Aguilar, C., Sun, M., Schulmann, K., Štípská, P., Jiang, Y., Yu, Y., Xiao, W., Wang, S. and Míková, J., 2018. Polycyclic Palaeozoic evolution of accretionary orogenic wedge in the southern Chinese Altai: evidence from structural relationships and U–Pb geochronology. Lithos, 314-315, 400-424.

Broussolle, A., Štípská, P., Lehmann, J., Schulmann, K., Hacker, B.R., Holder, R., Kylander-Clark, A.R.C., Hanžl, P., Racek, M., Hasalová, P., Lexa, O., Hrdličková, K. and Buriánek, D., 2015. P–T–t–D record of crustal-scale horizontal flow and magma-assisted doming in the SW Mongolian Altai. Journal of Metamorphic Geology, 33(4): 359-383.

Burenjargal, U., Okamoto, A., Kuwatani, T., Sakata, S., Hirata, T. and Tsuchiya, N., 2014. Thermal evolution of the Tseel terrane, SW Mongolia and its relation to granitoid intrusions in the Central Asian Orogenic Belt. Journal of Metamorphic Geology, 32(7)765-790.

Burenjargal, U., Okamoto, A., Meguro, Y. and Tsuchiya, N., 2012. An exhumation pressure–temperature path and fluid activities during metamorphism in the Tseel terrane, SW Mongolia: Constraints from aluminosilicate-bearing quartz veins and garnet zonings in metapelites. Journal of Asian Earth Sciences, 54: 214-229.

Buriánek, D., Schulmann, K., Hrdličková, K., Hanžl, P., Janoušek, V., Gerdes, A. and Lexa, O., 2017. Geochemical and geochronological constraints on distinct Early-Neoproterozoic and Cambrian accretionary events along southern margin of the Baydrag Continent in western Mongolia. Gondwana Research, 47: 200-227.

Burton, G.R., 2010. New structural model to explain geophysical features in northwestern New South Wales: implications for the tectonic framework of the Tasmanides. Australian Journal of Earth Sciences, 57(1): 23-49.

Buslov, M.M., Fujiwara, Y., Iwata, K. and Semakov, N.N., 2004. Late paleozoic-early Mesozoic geodynamics of Central Asia. gondwana Research, 7(3): 791-808.

Cai, K., Sun, M., Yuan, C., Long, X. and Xiao, W., 2011a. Geological framework and Paleozoic tectonic history of the Chinese Altai, NW China: a review. Russian Geology and Geophysics, 52(12): 1619-1633.

Cai, K., Sun, M., Yuan, C., Xiao, W., Zhao, G., Long, X. and Wu, F., 2012a. Carboniferous mantle-derived felsic intrusion in the Chinese Altai, NW China: Implications for geodynamic change of the accretionary orogenic belt. Gondwana Research, 22(2): 681-698.

Cai, K., Sun, M., Yuan, C., Zhao, G., Xiao, W. and Long, X., 2012b. Keketuohai mafic–ultramafic complex in the Chinese Altai, NW China: Petrogenesis and geodynamic significance. Chemical Geology, 294: 26-41.

Cai, K., Sun, M., Yuan, C., Zhao, G., Xiao, W., Long, X. and Wu, F., 2010. Geochronological and geochemical study of mafic dykes from the northwest Chinese Altai: Implications for petrogenesis and tectonic evolution. Gondwana Research, 18(4): 638-652.

Cai, K., Sun, M., Yuan, C., Zhao, G., Xiao, W., Long, X. and Wu, F., 2011b. Geochronology, petrogenesis and tectonic significance of peraluminous granites from the Chinese Altai, NW China. Lithos, 127(1): 261-281.

Cai, K., Sun, M., Yuan, C., Zhao, G., Xiao, W., Long, X. and Wu, F., 2011c. Prolonged magmatism, juvenile nature and tectonic evolution of the Chinese Altai, NW China: evidence from zircon U–Pb and Hf isotopic study of Paleozoic granitoids. Journal of Asian Earth Sciences, 42(5): 949-968.

Cawood, P.A., Hawkesworth, C.J. and Dhuime, B., 2012. Detrital zircon record and tectonic setting. Geology, 40(10): 875-878.

Chai, F., Mao, J., Dong, L., Yang, F., Liu, F., Geng, X. and Zhang, Z., 2009. Geochronology of metarhyolites from the Kangbutiebao Formation in the Kelang basin, Altay Mountains, Xinjiang: implications for the tectonic evolution and metallogeny. Gondwana Research, 16(2): 189-200.

Chai, F.M., Yang, F.Q., Liu, F., Geng, X.X., Jiang, L.P., Lv, S.J., Jiang., M., Zang., M. and Chen, B., 2012. Geochronology and genesis of meta- felsic volcanic rocks from the Kangbutiebao Formation in Chonghuer basin on southern margin of Altay, Xinjiang. Geological Review, 58(6): 1023–1037 (in Chinese with English abstract).

Chen, B. and Jahn, B.M., 2002. Geochemical and isotopic studies of the sedimentary and granitic rocks of the Altai orogen of northwest China and their tectonic implications. Geological Magazine, 139(1): 1-13.

Collins, W.J., Belousova, E.A., Kemp, A.I. and Murphy, J.B., 2011. Two contrasting Phanerozoic orogenic systems revealed by hafnium isotope data. Nature Geoscience, 4(5): 333-337.

Coney, P.J., Jones, D.L. and Monger, J.W.H., 1980. Cordilleran suspect terranes. Nature, 288(5789): 329-333.

Cox, K.G.E., Bell, J.D.. Pankhurst, R.J., 1979. The interpretation of igneous rocks. George Allen and Unwin, London, 450 pp.

Demoux, A., Kroner, A., Hegner, E. and Badarch, G., 2009. Devonian arc-related magmatism in the Tseel terrane of SW Mongolia: chronological and geochemical evidence. Journal of the Geological Society, 166(3): 459–471.

Dewey, J.F., 1977. Suture zone complexities: a review. Tectonophysics, 40(1-2): 53-67.

Edel, J.B., Schulmann, K., Hanžl, P. and Lexa, O., 2014. Palaeomagnetic and structural constraints on 90° anticlockwise rotation in SW Mongolia during the Permo–Triassic: Implications for Altaid oroclinal bending. Preliminary palaeomagnetic results. Journal of Asian Earth Sciences, 94(157-171).

Eizenhöfer, P.R., Zhao, G., Zhang, J. and Sun, M., 2014. Final closure of the Paleo- Asian Ocean along the Solonker Suture Zone: Constraints from geochronological and geochemical data of Permian volcanic and sedimentary rocks. Tectonics, 33(4): 441-463.

Fedo, C.M., Sircombe, K.N. and Rainbird, R.H., 2003. Detrital Zircon Analysis of the Sedimentary Record. Reviews in Mineralogy and Geochemistry, 53(1): 277-303.

Gao, F.P., Zhou, G., Lei, Y.X., Wang, D.S., Chen, J.X., Zhang, H.F., Wu, X.B., Liu, G.R. and Zhao, Z.H., 2010. Early Permian granite age and geochemical characteristics in Shaerbulake of Xinjiang's Altai area and it's geoloigcal significance. Geological Bulletin of China, 29(9): 1281-1293.

Gehrels, G., 2012. Detrital zircon U- Pb geochronology: Current methods and new opportunities. . Tectonics of sedimentary basins: Recent advances: 45-62.

Geng, X.X., Yang, F.Q., Chai, F.M., Liu, M., Guo, X.J., Guo, Z.L., Liu, F. and Zhang, Z.X., 2012. LA–ICP–MS U–Pb dating of volcanic rocks from Dadonggou ore district on southern margin of Altay in Xinjiang and its geological implications. Mineral Deposits, 31(5): 1119–1131 (in Chinese with English abstract).

Glen, J.M.G., Schmidt., J., Pellerin., L., McPhee., D.K. and O'Neill., J.M., 2007. Crustal structure of Wrangellia and adjacent terranes inferred from geophysical studies along a transect through the northern Talkeetna Mountains. Geol. Soc. Am. Spec. Pap., 431.

Grebennikov, A.V., 2014. A-type granites and related rocks: Petrogenesis and classification. Russian Geology and Geophysics 55, 1074-1086.

Guo, X.J., Li, Y., Kong, L.H., Zheng, J.H. and Sun, D.Q., 2015. Geological characteristics and metallogenesis of the Boketubayi iron–manganese deposit in Altay, Xinjiang. Geoscience, 29(6): 1309–1318 (in Chinese with English abstract).

Guy, A., Schulmann, K., Clauer, N., Hasalova, P., Seltmann, R., Armstrong, R., Lexa, O. and Benedicto, A., 2014a. Late Paleozoic–Mesozoic tectonic evolution of the Trans-Altai and South Gobi Zones in southern Mongolia based on structural and geochronological data. Gondwana Research, 25(1): 309-337.

Guy, A., Schulmann, K., Munschy, M., Miehe, J.M., Edel, J.B., Lexa, O. and Fairhead, D., 2014b. Geophysical constraints for terrane boundaries in southern Mongolia. Journal of Geophysical Research: Solid Earth, 119(10): 7966-7991.

Guy, A., Schulmann, K., Janoušek, V., Štípská, P., Armstrong, R., Belousova, E., Dolgopolova, E., Seltman, R., Lexa, O., Jiang. Y., & Hanžl, P. (2015). Geophysical and geochemical nature of relaminated arc- derived lower crust underneath oceanic domain in southern Mongolia. Tectonics, *34*(5): 1030-1053.

Hanžl, P., Schulmann, K., Janousek, V., Lexa, O., Hrdlickova, K., Jiang, Y., Buriánek, D., Altanbaatar, B., Ganchuluun, T. and Erban, V., 2016. Making continental crust: origin of Devonian orthogneisses from SE Mongolian Altai. Journal of GEOsciences, 61(1): 25-50.

He, H., 1990. Tectonic division and crustal evolution of Altay Orogenic Belt in china. Geoscience of Xinjiang, 2(9-20).

He, Y., Sun, M., Cai, K., Xiao, W., Zhao, G., Long, X. and Li, P., 2015. Petrogenesis of the Devonian high-Mg rock association and its tectonic implication for the Chinese Altai orogenic belt, NW China. Journal of Asian Earth Sciences, 113(0): 61-74.

Jahn, B.M., Windley, B., Natal'in, B. and Dobretsov, N.L., 2004. Phanerozoic continental growth in Central Asia. Journal of Asian Earth Sciences, 23(5): 599-603.

Jahn, B.M., Wu, F. and Chen, B., 2000a. Granitoids of the Central Asian Orogonic Belt and continental growth in the Phanerozoic. Transactions of the Royal Society of Edinburgh, Earth Sciences, 91(1–2): 181.

Jahn, B.M., Wu, F. and Chen, B., 2000b. Massive granitoid generation in Central Asia: Nd isotope evidence and implication for continental growth in the Phanerozoic. Episodes, 23(2): 82-92.

Janoušek, V., Farrow, C.M. and Erban, V., 2006. Interpretation of whole-rock geochemical data in igneous geochemistry: introducing Geochemical Data Toolkit (GCDkit). Journal of Petrology, 47(6): 1255-1259.

Janoušek, V., Jiang, Y., Buriánek, D., Schulmann, K., Hanžl, P., Soejono, I., Kröner, A., Altanbaatar, B., Erban, V., Lexa, O., Ganchuluun, T. and Košler, J., 2018. Cambrian–Ordovician magmatism of the Ikh-Mongol Arc System exemplified by the Khantaishir Magmatic Complex (Lake Zone, south–central Mongolia). Gondwana Research, 54: 122-149.

Janoušek, V., Jiang, Y., Schulmann, K., Buriánek, D., Hanzl, P., Lexa, O., Ganchuluun, T. and Battushig, A., 2014. The age, nature and likely genesis of the Cambrian Khantaishir arc, Lake Zone, Mongolia, EGU General Assembly Conference Abstracts, pp. 6108.

Jiang, Y.D., Sun, M., Zhao, G., Yuan, C., Xiao, W., Xia, X. and Wu, F., 2011. Precambrian detrital zircons in the Early Paleozoic Chinese Altai: their provenance and implications for the crustal growth of central Asia. Precambrian Research, 189(1): 140-154.

Jiang, Y.D., Schulmann, K., Sun, M., Weinberg, R.F., Štípská, P., Li, P.F., Zhang, J., Chopin, F., Wang, S., Xia, X.P., and Xiao, W.J., in review. Structural and geochronological constraints on Devonian supra-subduction tectonic switching and Permian collisional dynamics in the Chinese Altai, central Asia. Tectonics.

Jiang, Y.D., K. Schulmann, M. Sun, P. Štípská, A. Guy, V. Janoušek, O. Lexa and Yuan, C., 2016. Anatexis of accretionary wedge, Pacific-type magmatism, and formation of vertically stratified continental crust in the Altai Orogenic Belt,. Tectonics, 35: 3095–3118.

Jiang, Y.D., Schulmann, K., Kröner, A., Sun, M., Lexa, O., Janoušek, V., Buriánek, D., Yuan, C. and Hanžl, P., 2017. Neoproterozoic-Early Paleozoic Peri-Pacific Accretionary Evolution of the Mongolian Collage System: Insights From Geochemical and U–Pb Zircon Data From the Ordovician Sedimentary Wedge in the Mongolian Altai. Tectonics, 36(11): 2305-2331.

Jiang, Y.D., Štípská, P., Sun, M., Schulmann, K., Zhang, J., Wu, Q.H., Long, X.P., Yuan, C., Racek, M., Zhao, G.C. and Xiao, W.J., 2015. Juxtaposition of Barrovian and migmatite domains in the Chinese Altai: a result of crustal thickening followed by doming of partially molten lower crust. Journal of Metamorphic Geology, 33(1): 45-70.

Jiang, Y.D., Sun, M., Kröner, A., Tumurkhuu, D., Long, X.P., Zhao, G.C., Yuan, C. and Xiao, W.F., 2012. The high-grade Tseel Terrane in SW Mongolia: An Early Paleozoic arc system or a Precambrian sliver? Lithos, 142: 95–115.

Jiang, Y.D., Sun, M., Zhao, G.C., Yuan, C., Xiao, W., Xia, X.P., Long, X.P. and Wu, F.Y., 2010. The 390 Ma high-T metamorphic event in the Chinese Altai: A consequence of ridge-subduction? American Journal of Science, 310(10): 1421–1452.

Kovach, V., Yarmolyuk, V., Kovalenko, V., Kozlovskyi, A., Kotov, A. and Terent'eva, L., 2011. Composition, sources, and mechanisms of formation of the continental crust of the Lake zone of the Central Asian Caledonides. II. Geochemical and Nd isotope data. Petrology, 19(4): 399-425.

Kozakov, I.K., Didenko, A.N., Azimov, P.Y., Kirnozova, T.I., Sal'nikova, E.B., Anisimova, I.V. and Erdenejargal, C., 2011. Geodynamic settings and formation conditions of crystalline complexes in the south Altai and south Gobi metamorphic belts. Geotectonics, 45(3): 174-194.

Kruk, N.N., Kuibida, Ya.V., Shokalsky, S.P., Kiselev, V.I., Gusev, N.I., 2018. Late Cambrian - Early Ordovician turbidites of Gorny Altai (Russia): Compositions, sources, deposition settings, and tectonic implications. Journal of Asian Earth Sciences 159, 209-232

Laurent-Charvet, S., Charvet, J., Monié, P. and Shu, L., 2003. Late Paleozoic strike- slip shear zones in eastern Central Asia (NW China): New structural and geochronological data. Tectonics, 22(2).

Laurent-Charvet, S., Charvet, J., Shu, L., Ma, R. and Lu, H., 2002. Palaeozoic late collisional strike-slip deformations in Tianshan and Altay, Eastern Xinjiang, NW China. Terra Nova, , 14(4): 249-256.

Lehmann, J., Schulmann, K., Lexa, O., Corsini, M., Kröner, A., Štípská, P., Tomurhuu, D. and Otgonbator, D., 2010. Structural constraints on the evolution of the Central Asian Orogenic Belt in Southern Mongolia. American Journal of Science, 310(7): 575–628.

Lehmann, J., Schulmann, K., Lexa, O., Závada, P., Štípská, P., Hasalová, P., Belyanin, G. and Corsini, M., 2017. Detachment folding of partially molten crust in accretionary orogens: A new magma-enhanced vertical mass and heat transfer mechanism. Litosphere.

Li, P., Sun, M., Rosenbaum, G., Cai, K., Chen, M. and He, Y., 2016a. Transpressional deformation, strain partitioning and fold superimposition in the southern Chinese Altai, Central Asian Orogenic Belt. Journal of Structural Geology, 87: 64-80.

Li, P., Sun, M., Rosenbaum, G., Cai, K. and Yu, Y., 2015a. Structural evolution of the Irtysh Shear Zone (northwestern China) and implications for the amalgamation of arc systems in the Central Asian Orogenic Belt. Journal of Structural Geology, 80: 142-156.

Li, P., Sun, M., Rosenbaum, G., Jiang, Y. and Cai, K., 2016b. Structural evolution of zonal metamorphic sequences in the southern Chinese Altai and relationships to Permian transpressional tectonics in the Central Asian Orogenic Belt. Tectonophysics, 693: 277-289.

Li, P., Sun, M., Rosenbaum, G., Jourdan, F., Li, S. and Cai, K., 2017. Late Paleozoic closure of the Ob-Zaisan Ocean along the Irtysh shear zone (NW China): Implications for arc amalgamation and oroclinal bending in the Central Asian orogenic belt. Geological Society of America. Geological Society of America Bulletin, 129(5-6): 547.

Li, P., Yuan, C., Sun, M., Long, X. and Cai, K., 2015b. Thermochronological constraints on the late Paleozoic tectonic evolution of the southern Chinese Altai. Journal of Asian Earth Sciences, 113: 51-60.

Li, X.R., Liu, F. and Yang, F.Q., 2012. Geological times and its signification of the two mica syenogranite in the Keyinblak Cu-Zn deposit area in Altay, Xinjiang. Xinjiang Geology, 30(1): 5–11 (in Chinese with English Abstract).

Li, Z., Li, Y., Chen, H., Santosh, M., Xiao, W. and Wang, H., 2010. SHRIMP U–Pb zircon chronology of ultrahigh-temperature spinel–orthopyroxene–garnet granulite from South Altay orogenic belt, northwestern China. Island Arc, 19(3): 506-516.

Li, Z., Yang, X., Li, Y., Santosh, M., Chen, H. and Xiao, W., 2014. Late Paleozoic tectono–metamorphic evolution of the Altai segment of the Central Asian Orogenic Belt: Constraints from metamorphic P–T pseudosection and zircon U–Pb dating of ultra-high-temperature granulite. Lithos, 204: 83-96.

Liu, F., Li, Y.H., Mao, J.W., Yang, F.Q., Chai, F.M., Geng, X.X. and Yang, Z.X., 2008. The SHRIMP U–Pb ages of Abagong granites in the Altaid Orogen and its geologic implication. Acta Geoscientica Sinica, 29: 795-804.

Liu, W., Liu, L.J., Liu, X.J., Shang, H.J. and Zhou, G., 2010. Age of the Early Devonian Kangbutiebao Formation along the southern Altay Mountains and its northeastern extension. Acta Petrologica Sinica, 26(2): 387–400 (in Chinese with the English abstract).

Liu, W., Liu, X.J. and Xiao, W.J., 2012. Massive granitoid production without massive continental-crust growth in the Chinese Altay: Insight into the source rock of granitoids using integrated zircon U–Pb age, Hf-Nd-Sr isotopes and geochemistry. American Journal of Science, 312(6), 629-684. American Journal of Science, 312(6): 629-684.

Long, X., Sun, M., Yuan, C., Xiao, W. and Cai, K., 2008. Early Paleozoic sedimentary record of the Chinese Altai: Implications for its tectonic evolution. Sedimentary Geology, 208(3–4): 88-100.

Long, X., Sun, M., Yuan, C., Xiao, W., Lin, S., Wu, F. and Cai, K., 2007. Detrital zircon age and Hf isotopic studies for metasedimentary rocks from the Chinese Altai: Implications for

the Early Paleozoic tectonic evolution of the Central Asian Orogenic Belt. Tectonics, 26(5).

Long, X., Yuan, C., Sun, M., Xiao, W., Wang, Y., Cai, K. and Jiang, Y., 2012. Geochemistry and Nd isotopic composition of the Early Paleozoic flysch sequence in the Chinese Altai, Central Asia: Evidence for a northward-derived mafic source and insight into Nd model ages in accretionary orogen. Gondwana Research, 22(2): 554-566.

Long, X., Yuan, C., Sun, M., Xiao, W., Zhao, G., Wang, Y. and Xie, L., 2010. Detrital zircon ages and Hf isotopes of the early Paleozoic flysch sequence in the Chinese Altai, NW China: new constrains on depositional age, provenance and tectonic evolution. Tectonophysics, 480(1): 213-231.

Lou, F., 1997. Characteristics of late Caledonian granites in the Nuoerte area, Altay, China. Jiangxi Geology, 11(3): 60–66 (in Chinese with English abstract).

Mossakovsky, A.A., Ruzhentsev, S.V., Samygin, S.G. and Kheraskova, T.N., 1993. Central Asian fold belt: geodynamic evolution and history of formation. Geotectonics, 6: 3–33.

Nakano, N., Osanai, Y., Owada, M., Satish-Kumar, M., Adachi, T., Jargalan, S., Yoshimoto, A., Syeryekhan, K. and Boldbaatar, C.H., 2015. Multiplegrowth of garnet, sillimanite/kyanite and monazite during amphibolite-facies metamorphism: implications for the P–T–tand tectonic evolution of the western Altai Range, Mongolia. Journal of Metamorphic Geology, 33(9): 937-958.

Pavlis, N.K., Holmes., S.A., Kenyon., S.C. and Factor., J.K., 2012. The development and evaluation of the EarthGravitational Model 2008 (EGM2008). J. Geophys. Res., 117(B04406).

Peccerillo, A. and Taylor, S.R., 1976. Geochemistry of Eocene calk-alkaline volcanic rocks from the kastamonu area, northen Turkey. Contributions to Mineralogy and Petrology 58, 61-83.

Qu, G. and Zhang, J., 1994. Oblique thrust systems in the Altay orogen, China. Journal of Southeast Asian Earth Sciences 9, 277-287.

Rojas-Agramonte, Y., Kröner, A., Demoux, A., Xia, X., Wang, W., Donskaya, T., Liu, D. and Sun, M., 2011. Detrital and xenocrystic zircon ages from Neoproterozoic to Palaeozoic arc terranes of Mongolia: significance for the origin of crustal fragments in the Central Asian Orogenic Belt. Gondwana Research, 19(3): 751-763.

Sengör, A.M.C. and Dewey, J.F., 1990. Terranology: vice or virtue? Trans. R. Soc. Lond. A, 331(1620): 457-477.

Şengör, A.M.C. and Natal'in, B.A., 1996. Palaeotectonics of Asia: fragments of a synthesis. In: A. Yin and M. Harrison (Editors), The Tectonic Evolution of Asia. Cambridge, Cambridge University Press, pp. 486–640.

Şengör, A.M.C., Natal'in, B.A. and Burtman, V.S., 1993. Evolution of the Altaid tectonic collage and Paleozoic crustal growth in Eurasia. Nature, 364: 299–307.

Shan, Q., Zeng, Q.S., Luo, Y., Yang, W.B., Zhang, H., Qiu, Y.Z. and Yu, X.Y., 2011. SHRIMP U–Pb ages and petrology studies on the potassic and sodic rhyolites in Altai, North Xinjiang. Acta Petrologica Sinica, 27(12): 3653–3665 (in Chinese with English abstract).

Shand, S.J., 1943. Eruptive rocks: their genesis, composition, classification, and their relation to ore-deposits, with a chapter on meteorites. New York.

Soejono, I., Buriánek, D., Janoušek, V., Svojtka, M., Čáp, P., Erban, V. and Ganpurev, N., 2017. A reworked Lake Zone margin: Chronological and geochemical constraints from the

Ordovician arc-related basement of the Hovd Zone (western Mongolia). Lithos, 294: 112-132.

Soejono, I., Čáp, P; Míková, J., Janoušek, V., Buriánek, D., Schulmann, K, 2018. Early Palaeozoic sedimentary record and provenance of flysch sequences in the Hovd Zone (western Mongolia): Implications for the geodynamic evolution of the Altai accretionary wedge system. Gondwana Research, 64: 163–183.

Sun, M., Long, X., Cai, K., Jiang, Y., Wang, B., Yuan, C., Zhao, G., Xiao, W. and Wu, F., 2009. Early Paleozoic ridge subduction in the Chinese Altai: insight from the abrupt change in zircon Hf isotopic compositions. Science in China Series D: Earth Sciences, 52(9): 1345–1358.

Sun, M., Yuan, C., Xiao, W., Long, X., Xia, X., Zhao, G., Lin, S., Wu, F. and Kröner , A., 2008. Zircon U–Pb and Hf isotopic study of gneissic rocks from the Chinese Altai: progressive accretionary history in the early to middle Palaeozoic. Chemical Geology, 247(3): 352-383.

The Team One of Geology of Xinjiang, 1979. Four Unpublished Geological Maps of Altai, with Geological Report, scale 1/200,000.

Thompson, A. B., Schulmann, K., Jezek, J., & Tolar, V. (2001). Thermally softened continental extensional zones (arcs and rifts) as precursors to thickened orogenic belts. Tectonophysics, 332(1-2), 115-141.

Tong, L., Chen, Y., Xu, Y., Zhou, X. and Liu, Z., 2013. Zircon U–Pb ages of the ultrahigh-temperature metapelitic granulite from the Altai orogeny, NW China, and geological implications. Acta Petrol. Sin, 29: 3435-3445.

Tong, L., Xu, Y.-G., Cawood, P.A., Zhou, X., Chen, Y. and Liu, Z., 2014a. Anticlockwise P-T evolution at ~280Ma recorded from ultrahigh-temperature metapelitic granulite in the Chinese Altai orogenic belt, a possible link with the Tarim mantle plume? Journal of Asian Earth Sciences, 94(0): 1-11.

Tong, Y., Wang, T., Hong, D., Dai, Y.J., Han, B.F. and Liu, X.M., 2007. Age and origin of the early Devonian granites from the north part of the Chinese Altai Moutains and its tectonic implications. Acta Geologica Sinica, 23(8): 1933-1944.

Tong, Y., Wang, T. and Hong, D.W., 2005. Zircon U–Pb age of syn-orogenic Tielieke pluton in the western part of Altay orogenic belt and its structural implications. Acta Geoscientica Sinica, 26(1): 74–77 (Chinese with English abstract).

Tong, Y., Wang, T., Jahn, B.M., Sun, M., Hong, D.W. and Gao, J.F., 2014b. Post-accretionary permian granitoids in the Chinese Altai orogen: Geochronology, petrogenesis and tectonic implications. American Journal of Science, 314(1): 80-109.

Tong, Y., Wang, T., Siebel, W., Hong, D.-W. and Sun, M., 2012. Recognition of early Carboniferous alkaline granite in the southern Altai orogen: post-subduction processes constrained by U–Pb zircon ages, Nd isotopes, and geochemical data. International Journal of Earth Sciences, 101(4): 937-950.

Wan, B., Xiao, W., Zhang, L., Windley, B.F., Han, C. and Quinn, C.D., 2011. Contrasting styles of mineralization in the Chinese Altai and East Junggar, NW China: implications for the accretionary history of the southern Altaids. Journal of the Geological Society, 168(6), 1311-1321. journal of the Geological Society, 168(6): 1311-1321.

Wang, T., Hong, D.W., Jahn, B.M., Tong, Y., Wang, Y.B., Han, B.F. and Wang, X.X., 2006. Timing, petrogenesis, and setting of Paleozoic synorogenic intrusions from the Altai

Mountains, Northwest China: implications for the tectonic evolution of an accretionary orogen. The Journal of Geology, 114(6): 735-751.

Wang, T., Jahn, B.M., Kovach, V.P., Tong, Y., Hong, D.W. and Han, B.F., 2009a. Nd–Sr isotopic mapping of the Chinese Altai and implications for continental growth in the Central Asian Orogenic Belt. Lithos, 110(1): 359-372.

Wang, T., Jahn, B.M., Kovach, V.P., Tong, Y., Wilde, S.A., Hong, D.W., Li, S. and Salnikova, E.B., 2014a. Mesozoic intraplate granitic magmatism in the Altai accretionary orogen, NW China: Implications for the orogenic architecture and crustal growth. American Journal of Science, 314(1): 1-42.

Wang, W., Wei, C., Wang, T., Lou, Y. and Chu, H., 2009b. Confirmation of pelitic granulite in the Altai orogen and its geological significance. Chinese Science Bulletin, 54(14): 2543-2548.

Wang, W., Wei, C., Zhang, Y., Chu, H., Zhao, Y. and Liu, X., 2014b. Age and origin of sillimanite schist from the Chinese Altai metamorphic belt: implications for late Palaeozoic tectonic evolution of the Central Asian Orogenic Belt. International Geology Review, 56(2): 224-236.

Wang, Y., Long, X., Wilde, S.A., Xu, H., Sun, M., Xiao, W., Yuan, C. and Cai, K., 2014c. Provenance of Early Paleozoic metasediments in the central Chinese Altai: Implications for tectonic affinity of the Altai-Mongolia terrane in the Central Asian Orogenic Belt. Lithos, 210–211(0): 57-68.

Wang, Z.G. and Zhao, Z.H., 1998. Geochemistry of the Granitoids in Altay. . Science Press, Beijing: 1–152 (in Chinese with English abstract).

Wei, C., Clarke, G., Tian, W. and Qiu, L., 2007. Transition of metamorphic series from the Kyanite-to andalusite-types in the Altai orogen, Xinjiang, China: Evidence from petrography and calculated KMnFMASH and KFMASH phase relations. Lithos, 96(3): 353-374.

Wilhem, C., Windley, B.F. and Stampfli, G.M., 2012. The Altaids of Central Asia: A tectonic and evolutionary innovative review. Earth-Science Reviews, 113(3): 303-341.

Windley, B.F., Alexeiev, D., Xiao, W., Kroner, A. and Badarch, G., 2007. Tectonic models for accretion of the Central Asian Orogenic Belt. Journal of the Geological Society, 164(1): 31–47.

Windley, B.F., Kroener, A., Guo, J., Qu, G., Li, Y. and Zhang, C., 2002. Neoproterozoic to Paleozoic Geology of the Altai Orogen, NW China: New Zircon Age Data and Tectonic Evolution. The Journal of Geology, 110: 719–737.

Xiao, W., Huang, B., Han, C., Sun, S. and Li, J., 2010. A review of the western part of the Altaids: a key to understanding the architecture of accretionary orogens. Gondwana Research, 18(2): 253-273.

Xiao, W., Windley, B., Sun, S., Li, J., Huang, B., Han, C., Yuan, C., Sun, M. and Chen, H., 2015. A Tale of Amalgamation of Three Permo-Triassic Collage Systems in Central Asia: Oroclines, Sutures, and Terminal Accretion. Annual Review of Earth and Planetary Sciences, 43(1): 477-507.

Xiao, W., Windley, B.F., Badarch, G., Sun, S., Li, J., Qin, K. and Wang, Z., 2004. Palaeozoic accretionary and convergent tectonics of the southern Altaids: implications for the growth of Central Asia. Journal of the Geological Society, 161(13): 339-342.

Xiao, W.J., Windley, B.F., Yuan, C., Sun, M., Han, C.M., Lin, S.F. and Sun, S., 2009. Paleozoic multiple subduction-accretion processes of the southern Altaids. . American Journal of Science, 309(3): 221-270.

Yan, S., Chen, W., Wang, Y., Zhang, Z. and Chen, B., 2004. 40Ar/39Ar dating and its significance of the Ertix gold metallogenic belt in the Altay orogen, Xinjiang. 地质学报.

Yang, C., Yang, F., Chai, F. and Wu, Y., 2017. Timing of formation of the Keketale Pb–Zn deposit, Xinjiang, Northwest China, Central Asian Orogenic Belt: Implications for the metallogeny of the South Altay Orogenic Belt. Geological Journal.

Yang, F., Mao, J., Liu, F., Chai, F., Guo, Z., Zhou, G. and Gao, J., 2010. Geochronology and geochemistry of the granites from the Mengku iron deposit, Altay Mountains, northwest China: implications for its tectonic setting and metallogenesis. Australian Journal of Earth Sciences,, 57(6): 803-818.

Yang, T.N., Li, J.Y., Zhang, J.E. and Hou, K.J., 2011. The Altai-Mongolia terrane in the Central Asian Orogenic Belt (CAOB): A peri-Gondwana one? Evidence from zircon U–Pb, Hf isotopes and REE abundance. Precambrian Research, 187(1): 79-98.

Yarmolyuk, V., Kovach, V., Kovalenko, V., Salnikova, E., Kozlovskii, A., Kotov, A., Yakovleva, S. and Fedoseenko, A., 2011. Composition, sources, and mechanism of continental crust growth in the Lake zone of the Central Asian Caledonides: I. Geological and geochronological data. Petrology, 19(1): 55-78.

Yu, Y., Sun, M., Long, X., Li, P., Zhao, G., Kröner, A., Broussolle, A. and Yang, J., 2017. Whole-rock Nd–Hf isotopic study of I-type and peraluminous granitic rocks from the Chinese Altai: Constraints on the nature of the lower crust and tectonic setting. Gondwana Research, 47: 131-141.

Yuan, C., Sun, M., Xiao, W., Li, X., Chen, H., Lin, S., Xia, X. and Long, X., 2007. Accretionary orogenesis of the Chinese Altai: insights from Paleozoic granitoids. Chemical Geology, 242(1): 22–39.

Yuan, F., Zhou, T.F. and Yue, S.C., 2001. The ages and the genetics types of the granites in the Nurt area, Altay. Xijiang Geology, 4(17): (In chinese abstract in english).

Zhang, C.-L., Li, Z.-X., Li, X.-H., Xu, Y.-G., Zhou, G. and Ye, H.-M., 2010. A Permian large igneous province in Tarim and Central Asian orogenic belt, NW China: Results of a ca. 275 Ma mantle plume? Geological Society of America Bulletin: B30007. 1.

Zhang, C., Liu, L., Santosh, M., Luo, Q. and Zhang, X., 2017a. Sediment recycling and crustal growth in the Central Asian Orogenic Belt: Evidence from Sr–Nd–Hf isotopes and trace elements in granitoids of the Chinese Altay. Gondwana Research, 47(Supplement C): 142-160.

Zhang, C., Wei, C. and Hou, R., 2007. Phase equilibrium of low- pressure metamorphism in the Altai, Xinjiang, [in Chinese with English abstract]. Geol. China, 34(1): 34–41.

Zhang, C.L., Santosh, M., Zou, H.B., Xu, Y.G., Zhou, G., Dong, Y.G. and Wang, H.Y., 2012. Revisiting the "Irtish tectonic belt": Implications for the Paleozoic tectonic evolution of the Altai orogen. Journal of Asian Earth Sciences, 52(117-133).

Zhang, H., Niu, H., Terada, K., Yu, X., Sato, H. and Ito, J.i., 2003. Zircon SHRIMP U–Pb dating on plagiogranite from Kuerti ophiolite in Altay, North Xinjiang. Chinese Science Bulletin, 48(20): 2231-2235.

Zhang, J., Sun, M., Schulmann, K., Zhao, G., Wu, Q., Jiang, Y., Guy, A. and Wang, Y., 2015. Distinct deformational history of two contrasting tectonic domains in the Chinese Altai:

Their significance in understanding accretionary orogenic process. Journal of Structural Geology, 73: 64-82.

Zhang, J., Wang, J. and Ding, R., 2000. Characteristics and U–Pb ages of zircon in metavolcanics from the Kangbutiebao Formation in the Altay orogen, Xinjiang. Regional Geology of China, 19(3): 281-287.

Zhang, J., Wang, T., Tong, Y., Zhang, Z., Song, P., Zhang, L., Huang, H., Guo, L. and Hou, Z., 2017b. Tracking deep ancient crustal components by xenocrystic/inherited zircons of Palaeozoic felsic igneous rocks from the Altai–East Junggar terrane and adjacent regions, western Central Asian Orogenic Belt and its tectonic significance. International Geology Review, 59(16): 2021-2040.

Zhang, Z., Yan, S., Chen, B., Zhou, G., He, Y., Chai, F., He, L. and Wan, Y., 2006. SHRIMP zircon U–Pb dating for subduction-related granitic rocks in the northern part of east Jungaar, Xinjiang. Chinese Science Bulletin, 51(8): 952-962.

Zhao, Z.H., Wang, Z.G., Zou, T. and Masuda, A., 1993. The REE, isotopic composition of O, Pb, Sr and Nd and petrogenesis of granitoids in the Altai region. Progress of solid-earth sciences in northern Xinjiang, China. Science Press, Beijing: 239-266.

Zheng, C.Q., Kato, T., Enami, M. and Xu, X.C., 2007. CHIME monazite ages of metasediments from the Altai orogen in northwestern China: Devonian and Permian ages of metamorphism and their significance. Island Arc, 16(4): 598-604.

Zheng, J., Chai, F. and Yang, F., 2016 The 401–409 Ma Xiaodonggou granitic intrusion: implications for understanding the Devonian Tectonics of the Northwest China Altai orogen. International Geology Review, 58(5): 540-555.

Zhou, G., Zhang, Z., Wang, X.-k., Wang, X., Luo, S., He, B. and Zhang, X., 2007. Zircon U–Pb SHRIMP and 40Ar-39Ar dating of the granitic mylonite in the Mayinebo fault belt of north Xinjiang and its geological significance. Acta Geologica Sinica, 81(3): 359-369.

Zhou, G., Zhang, Z.C., Zhang, X.L., Luo., S.B., Yang, W.P., Gu, G.Z. and Wang, X., 2005. Discovery of Metabasic Rocks at the South Side of Mayinebo Fault in the South Margin of Altay Mountains, Xinjiang, and Its Geological Implications. Earth Science-Journal of China University of Geosciences, 30(6): 738–746.

Zhu, Y.F., Zeng, Y. and Gu, L., 2006. Geochemistry of the rare metal-bearing pegmatite No. 3 vein and related granites in the Keketuohai region, Altay Mountains, northwest China. journal of Asian Earth Sciences, 27(1): 61-77.

Zhuang, Y., 1994. The PTst Evolution of Metamorphism and Development Mechanism of the Thermal - Structural - Gneiss Domes in the Chinese Altaides. Acta Geologica Sinica, 7(3): 267-281.

Arnaud Broussolle is a Phd student at the University of Hong Kong (HKU), China. He obtained his Bachelor (2011) and Master (2013) degree from the University of Strasbourg (UDS), France. He was a research assistant at the Czech Geological Survey, Czech Republic during one year in 2014. He worked on doming structure and metamorphism of the Gobi Altai in Mongolia during his master thesis. His focuses are metamorphism, structural geology and geochronology of the Central Asian Orogenic Belt. His Ph.D. subject is about the understanding of a Permian tectono-thermal event in the Chinese Altai linked with the final closure of CAOB in the Central part.

Min Sun is a Professor at the Department of Earth Sciences, the University of Hong Kong (HKU), China. He graduated with a B.Sc. degree from Peking University in 1982, then went to the University of British Columbia in Vancouver, Canada, where he obtained his M.Sc. degree in 1985 and his Ph.D. in 1991. From 1991 to 1994 he was a Postdoctoral Research Fellow at the University of Saskatchewan, Saskatoon, Canada, and joined the University of Hong Kong in 1994 as Lecturer, later Associate Professor. He received a Collaborative Research Award for Outstanding Young Researchers in Hong Kong from the National Natural Science Foundation of China in 1999 and an Outstanding Young Researcher Award of HKU in 2001. He is a member of the Editorial Boards of Precambrian Research, Geochimica et Cosmochimica Acta, and Acta Geoscientia Sinica. His research focusses on the application of zircon U–Pb and Hf isotopic compositions to the evolution of the North China Craton and the South China Block as well as the Chinese and Mongolian Altai.

Karel Schulmann is an exceptional class Professor of geology at the University of Strasbourg, France and head of Centre for Lithospheric Research at the Czech Geological Survey, Czech Republic. He studied geology at Charles University in Prague, Czech Republic where he obtained his Ph.D. degree in 1987 and habilitation in 1991. From 2001 until 2004, he worked as a professor and the head of the Department of Petrology & Structural Geology, Charles University, Prague, Czech Republic. From 2004 until now, he is a professor at the University of Strasbourg (former University Louis Pasteur), France. Since 2012's he joined also the Czech Geological Survey, Prague, Czech Republic where he acts as the director of a research center and where he was appointed a national research grant for the study of the accretionary and collisional Paleozoic systems. He is an editor of International Journal of Earth Sciences, Journal of the Geological Society of London and associated editor of Tectonics and Terra Nova. He is a member of an Editorial Review Boards of several national journals (Slovakia, Russia, Czech Republic, France). His main research interests are geodynamics, tectonics and structural geology of accretionary and collisional orogenic belts.

Alexandra Guy is a researcher in geophysics and geology at the Centre for Lithospheric Research hosted by the Czech Geological Survey in Prague, Czech Republic. She studied geophysics and geology at the University of Strasbourg and Ecole et Observatoire des Sciences de la Terre (EOST) where she obtained her Ph.D. degree in 2012. From 2013 until now, she works as a researcher in Prague. Her main research interests are the geophysical and geological characterization of accretionary and collisional orogenic systems using gravity and magnetic data combined with structural and tectonic analyses. She is a member of the editorial board of the Journal of GEOsciences.

Carmen Aguilar is a Postdoctoral Research Fellow at the Centre for Lithospheric Research hosted by the Czech Geological Survey (ČGS) in Prague (Czech Republic). She obtained her B.Sc. degree in Geology at the University of Granada (1999-2005) and she completed her Ph.D. degree in 2013 at the University of Barcelona (Spain, respectively). The main goal of her thesis was to contribute to the understanding of the dynamics of the lithosphere and the origin of thermal anomalies in orogenic regimes through integrated structural, petrological and geochronological studies together with thermodynamic modeling in medium- to high-grade metamorphic rocks and in associated igneous rocks of the Variscan segment of the Pyrenees (France-Spain). From 2014 to 2016, she was a Postdoctoral Research Fellow at the Department of Earth Sciences of Universidade Federal de Ouro Preto (Brasil), where she worked on U–Pb titanite and monazite dating of the Transamazonian metamorphic event in the southern São Francisco Craton (Brazil). From 2017 until now, she works as a postdoc in the ČGS, where is working on projects related to the European Variscides and Central Asian Orogenic Belt. She is an expert in metamorphic petrology and geochronology.

Pavla Štípská is a Lecturer of Metamorphic petrology at the University of Strasbourg, France and a research geologist at the Czech Geological Survey, Czech Republic. She studied geology at Charles University in Prague, Czech Republic where she obtained her Ph.D. degree in 1999. From 1994 until 2005, she worked as researcher and lecturer of metamorphic petrology at the Department of Petrology & Structural Geology, Charles University, Prague, Czech Republic. From 2005 until now, she is a lecturer at the University of Strasbourg (former University Louis Pasteur), France, where she obtained Habilitation in 2011. Since 2012, she joined also the Czech Geological Survey, Prague, Czech Republic where she works as a research geologist and where she undertakes many research projects. She is a member of the Editorial Review Board of the Journal of Metamorphic

Geology. Her main research interests are metamorphism in the context of orogens, linking metamorphism with structural development and monazite and zircon geochronology, methods for modelling and constraining the P-T evolution of metamorphic rocks, the interpretation of reaction textures in metamorphic rocks, and partial melting of crustal rocks.

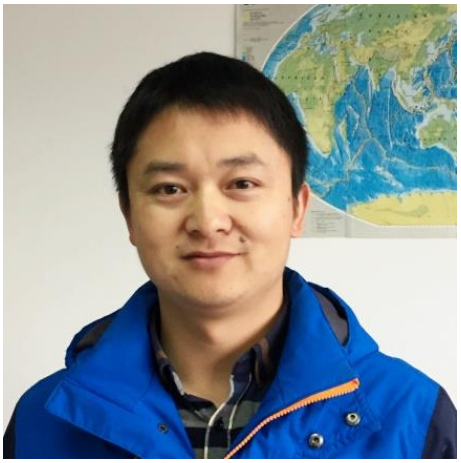

Yingde Jiang is a research professor at the Guangzhou Institute of Geochemistry, Chinese Academy of Sciences (GIG-CAS). He studied petrology and tectonic at the Department of Earth Sciences, the University of Hong Kong (HKU), where he obtained his Ph.D. degree in 2011. He was a Postdoctoral Research Fellow at HKU from 2011 to 2013, and at Charles University, Prague, Czech Republic, from 2013 till 2015, respectively. From 2015 till now, he works as a research professor in the GIG-CAS in the frame of "100 Talents" program of the CAS. He has mainly worked on the geology of the Chinese and Mongolian Altai Orogenic Belts since 2007. His current research interests focuses on the tectono-thermal evolution of the Chinese and Mongolian Altai by integrating critical information from structural geology, metamorphic petrology and phase equilibrium modelling, geochronology and geochemistry.

Yang Yu is a Postdoctoral Research Fellow at the Guangzhou Institute of Geochemistry, Chinese Academy of Sciences. He obtained his B.Sc. degree from the Chang'an University and Ph.D from the University of Hong Kong in 2017. His research interests are the petrogenesis of felsic and mafic rocks during orogeny and their implications for the crustal growth and differentiation.

Wenjiao Xiao is Vice Director and professor at the Xinjiang Institute of Ecology and Geography, Chinese Academy of Sciences (CAS) and professor at the Institute of Geology and Geophysics, CAS. He got his Ph.D. from the Institute of Geology, CAS, in 1995. He is now a GSA fellow, and is/was associate editors or on the editorial boards of Geological Society of America Bulletin, Journal of the Geological Society, Episodes, International Journal of Earth Sciences, Journal of Asian Earth Sciences, Gondwana Research, and Terra Nova. Wenjiao got the second award of National Natural Science Award of China in 2012, the first award of Science and Technology Award of Xinjiang Uyghur Autonomous Region, China in 2012, and the Huang Jiqing Award of the Geological Society of China in 2010. Wenjiao was/is a Co-chief of IGCP 592 and IGCP 662. His research interests include tectonic evolution of the orogenic belts and continental growth.

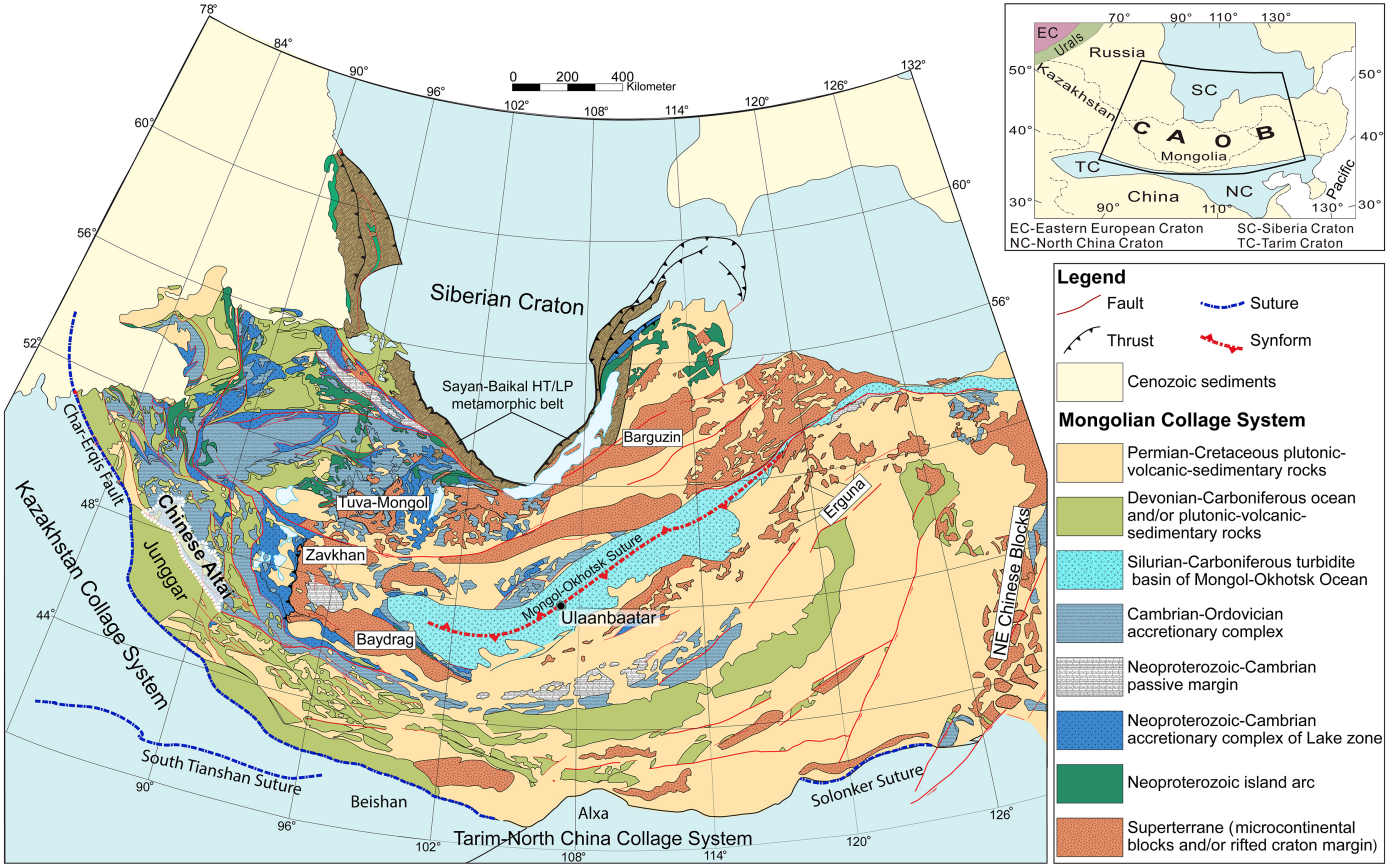
Siberian Craton
Sayan-Baikal HT/LP metamorphic belt
Barguzin
Tuva-Mongol
Zavkhan
Baydrag
Mongol-Okhotsk Suture
Ulaanbaatar
Erguna
NE Chinese Blocks
Char-Erqis Fault
Kazakhstan Collage System
Junggar
Chinese Altai
South Tianshan Suture
Beishan
Alxa
Tarim-North China Collage System
Solonker Suture
0 200 400 Kilometer
EC
Urals
Russia
Kazakhstan
SC
C A O B
Mongolia
TC
China
NC
Pacific
EC-Eastern European Craton
SC-Siberia Craton
NC-North China Craton
TC-Tarim Craton
Legend
Fault
Suture
Thrust
Synform
Cenozoic sediments
Mongolian Collage System
Permian-Cretaceous plutonic-volcanic-sedimentary rocks
Devonian-Carboniferous ocean and/or plutonic-volcanic-sedimentary rocks
Silurian-Carboniferous turbidite basin of Mongol-Okhotsk Ocean
Cambrian-Ordovician accretionary complex
Neoproterozoic-Cambrian passive margin
Neoproterozoic-Cambrian accretionary complex of Lake zone
Neoproterozoic island arc
Superterrane (microcontinental blocks and/or rifted craton margin)

Figure 1

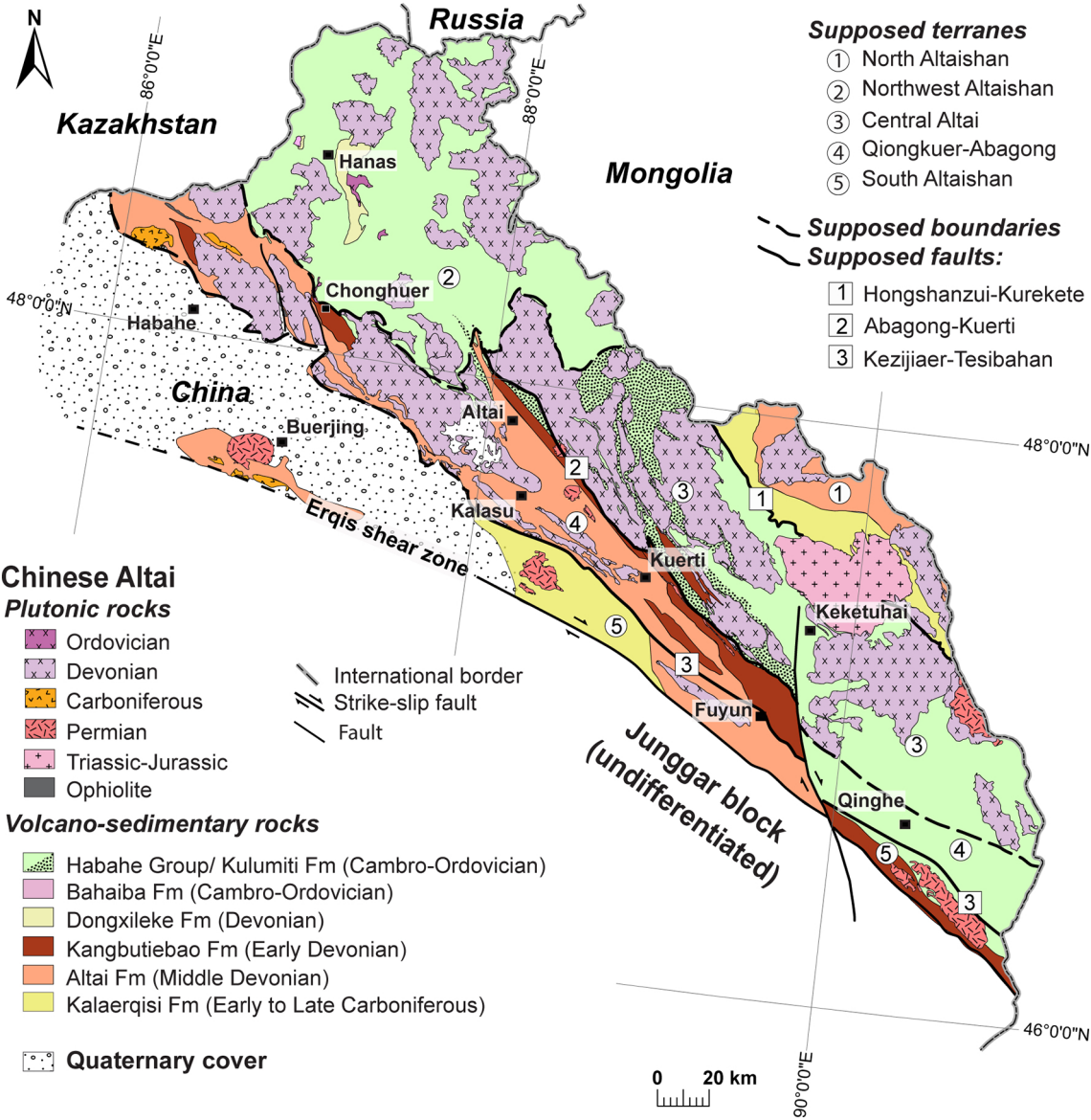
N
Russia
Kazakhstan
Mongolia
China
86°0'0"E
88°0'0"E
90°0'0"E
48°0'0"N
46°0'0"N
Hanas
Chonghuer
Habahe
Buerjing
Altai
Kalasu
Kuerti
Keketuhai
Fuyun
Qinghe
Erqis shear zone
Junggar block
(undifferentiated)
Supposed terranes
1 North Altaishan
2 Northwest Altaishan
3 Central Altai
4 Qiongkuer-Abagong
5 South Altaishan
Supposed boundaries
Supposed faults:
1 Hongshanzui-Kurekete
2 Abagong-Kuerti
3 Kezijiaer-Tesibahan
Chinese Altai
Plutonic rocks
Ordovician
Devonian
Carboniferous
Permian
Triassic-Jurassic
Ophiolite
International border
Strike-slip fault
Fault
Volcano-sedimentary rocks
Habahe Group/ Kulumiti Fm (Cambro-Ordovician)
Bahaiba Fm (Cambro-Ordovician)
Dongxileke Fm (Devonian)
Kangbutiebao Fm (Early Devonian)
Altai Fm (Middle Devonian)
Kalaerqisi Fm (Early to Late Carboniferous)
Quaternary cover
0 20 km

Figure 2

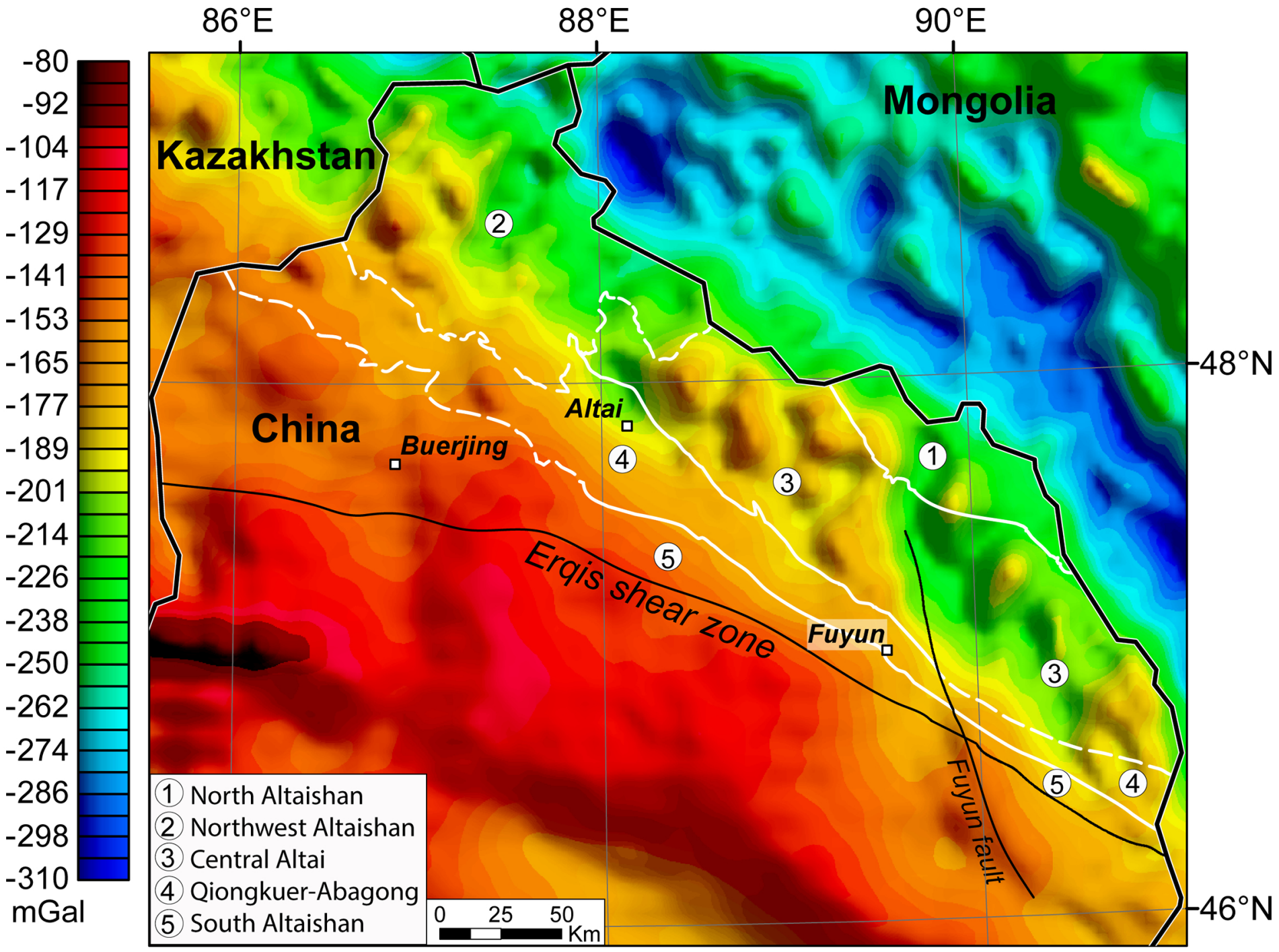
86°E
88°E
90°E
48°N
46°N
-80
-92
-104
-117
-129
-141
-153
-165
-177
-189
-201
-214
-226
-238
-250
-262
-274
-286
-298
-310
mGal
Kazakhstan
Mongolia
China
Altai
Buerjing
Fuyun
Erqis shear zone
Fuyun fault
1 North Altaishan
2 Northwest Altaishan
3 Central Altai
4 Qiongkuer-Abagong
5 South Altaishan
0 25 50
Km

Figure 3

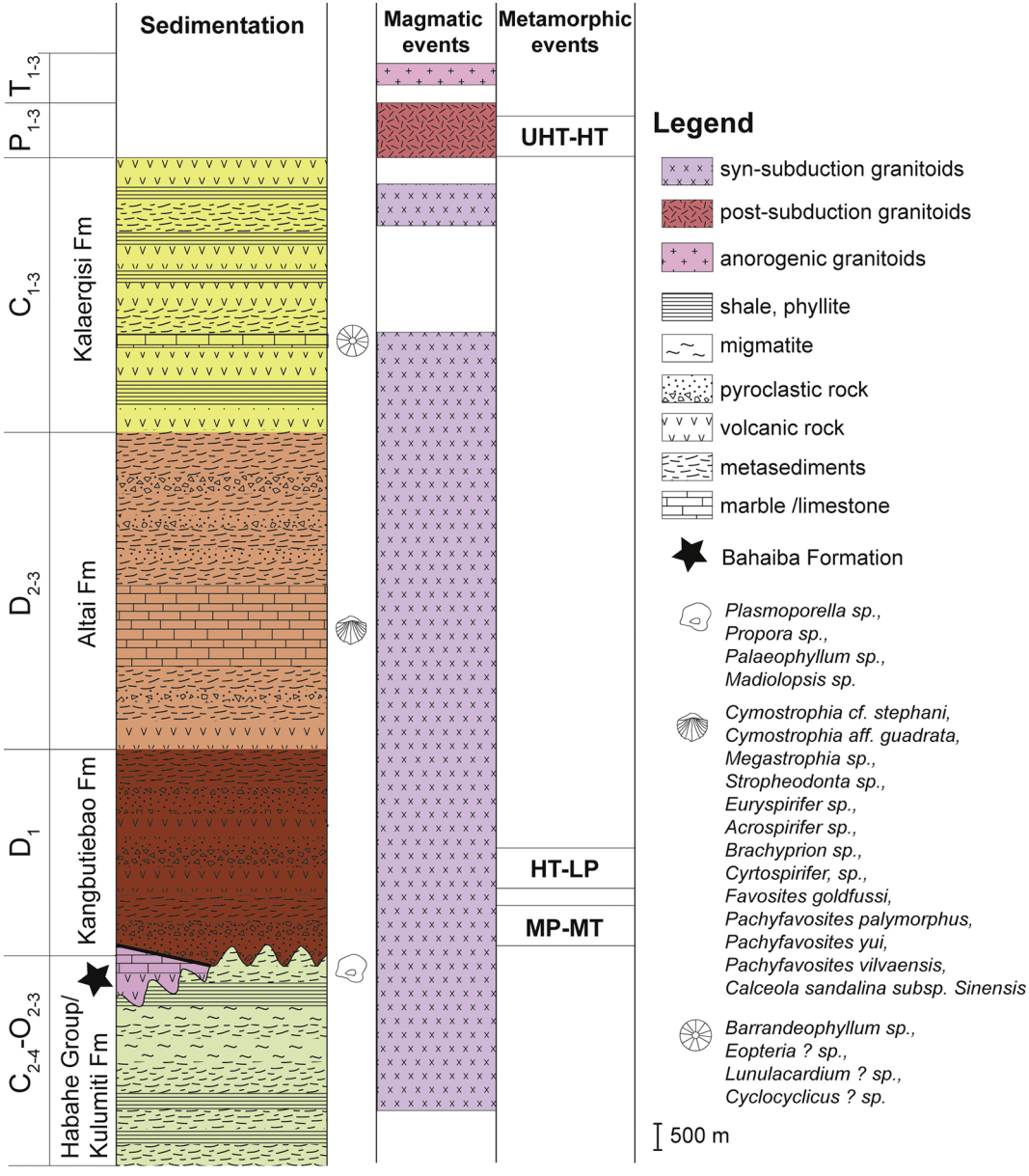
Sedimentation
Magmatic events
Metamorphic events
T1-3
P1-3
C1-3
Kalaerqisi Fm
D2-3
Altai Fm
D1
Kangbutiebao Fm
C2-4-O2-3
Habahe Group/ Kulumiti Fm
UHT-HT
HT-LP
MP-MT
Legend
syn-subduction granitoids
post-subduction granitoids
anorogenic granitoids
shale, phyllite
migmatite
pyroclastic rock
volcanic rock
metasediments
marble /limestone
Bahaiba Formation
Plasmoporella sp.,
Propora sp.,
Palaeophyllum sp.,
Madiolopsis sp.
Cymostrophia cf. stephani,
Cymostrophia aff. guadrata,
Megastrophia sp.,
Stropheodonta sp.,
Euryspirifer sp.,
Acrospirifer sp.,
Brachyprion sp.,
Cyrtospirifer, sp.,
Favosites goldfussi,
Pachyfavosites palymorphus,
Pachyfavosites yui,
Pachyfavosites vilvaensis,
Calceola sandalina subsp. Sinensis
Barrandeophyllum sp.,
Eopteria ? sp.,
Lunulacardium ? sp.,
Cyclocyclicus ? sp.
500 m

Figure 4

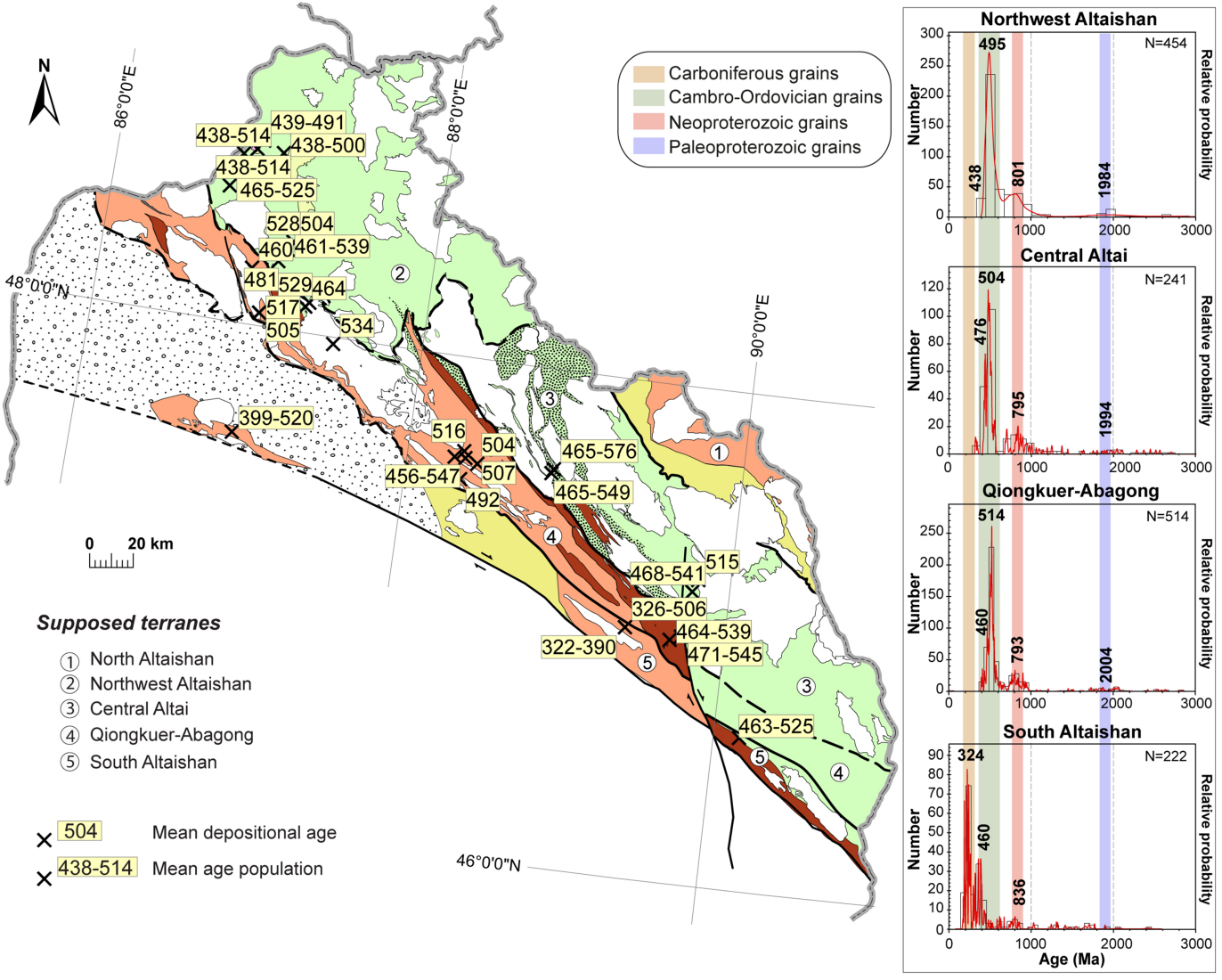
N
86°0'0"E
88°0'0"E
90°0'0"E
48°0'0"N
46°0'0"N
Carboniferous grains
Cambro-Ordovician grains
Neoproterozoic grains
Paleoproterozoic grains
438-514
439-491
438-500
438-514
465-525
528504
460
461-539
481
529
464
517
505
534
399-520
516
504
507
456-547
492
465-576
465-549
468-541
515
326-506
464-539
322-390
471-545
463-525
0 20 km
Supposed terranes
① North Altaishan
② Northwest Altaishan
③ Central Altai
④ Qiongkuer-Abagong
⑤ South Altaishan
504 Mean depositional age
438-514 Mean age population
Northwest Altaishan
N=454
495
438
801
1984
Central Altai
N=241
504
476
795
1994
Qiongkuer-Abagong
N=514
514
460
793
2004
South Altaishan
N=222
324
460
836
Number
Relative probability
Age (Ma)

Figure 5

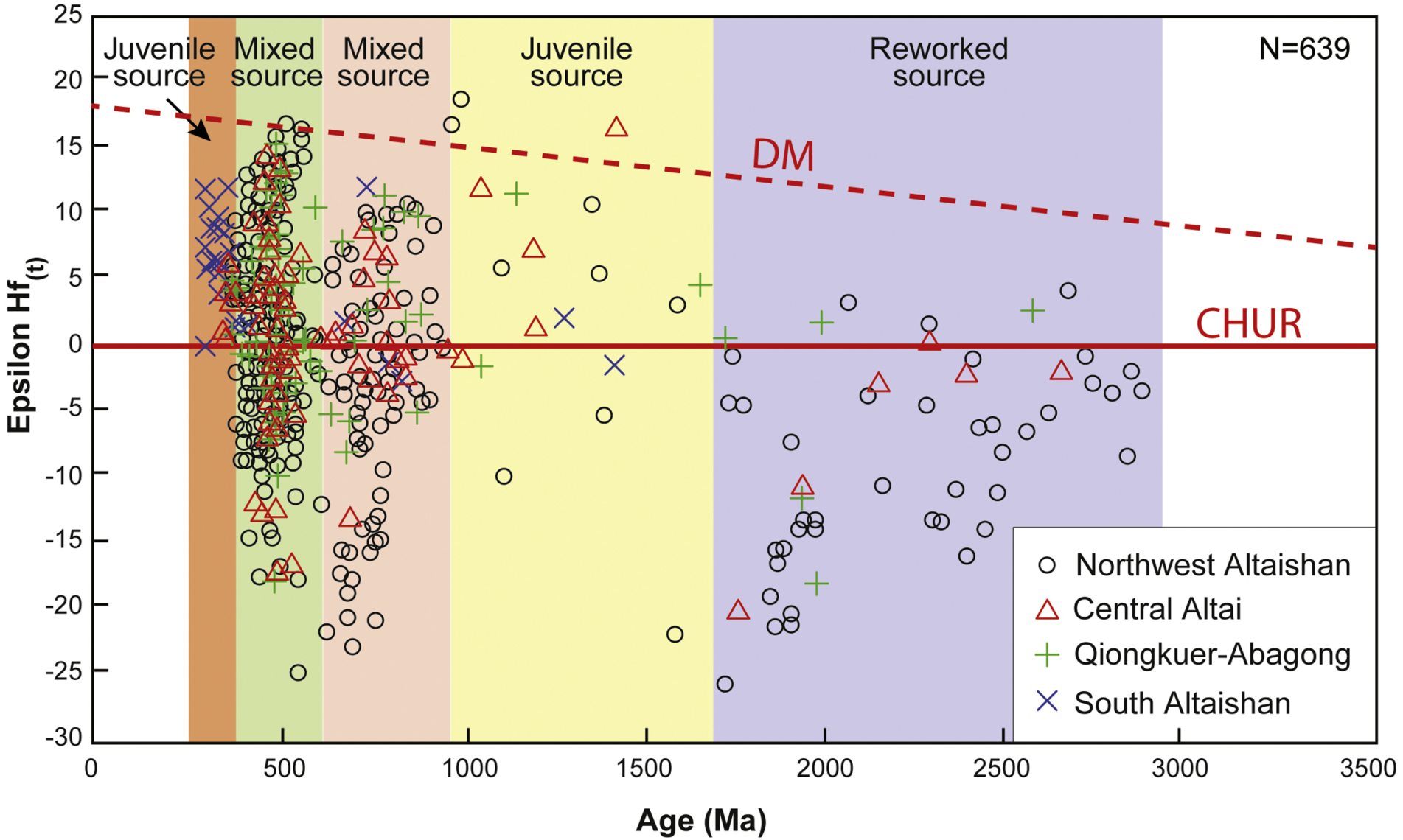
Juvenile source
Mixed source
Mixed source
Juvenile source
Reworked source
N=639
DM
CHUR
Epsilon Hf(t)
Age (Ma)
Northwest Altaishan
Central Altai
Qiongkuer-Abagong
South Altaishan

Figure 6

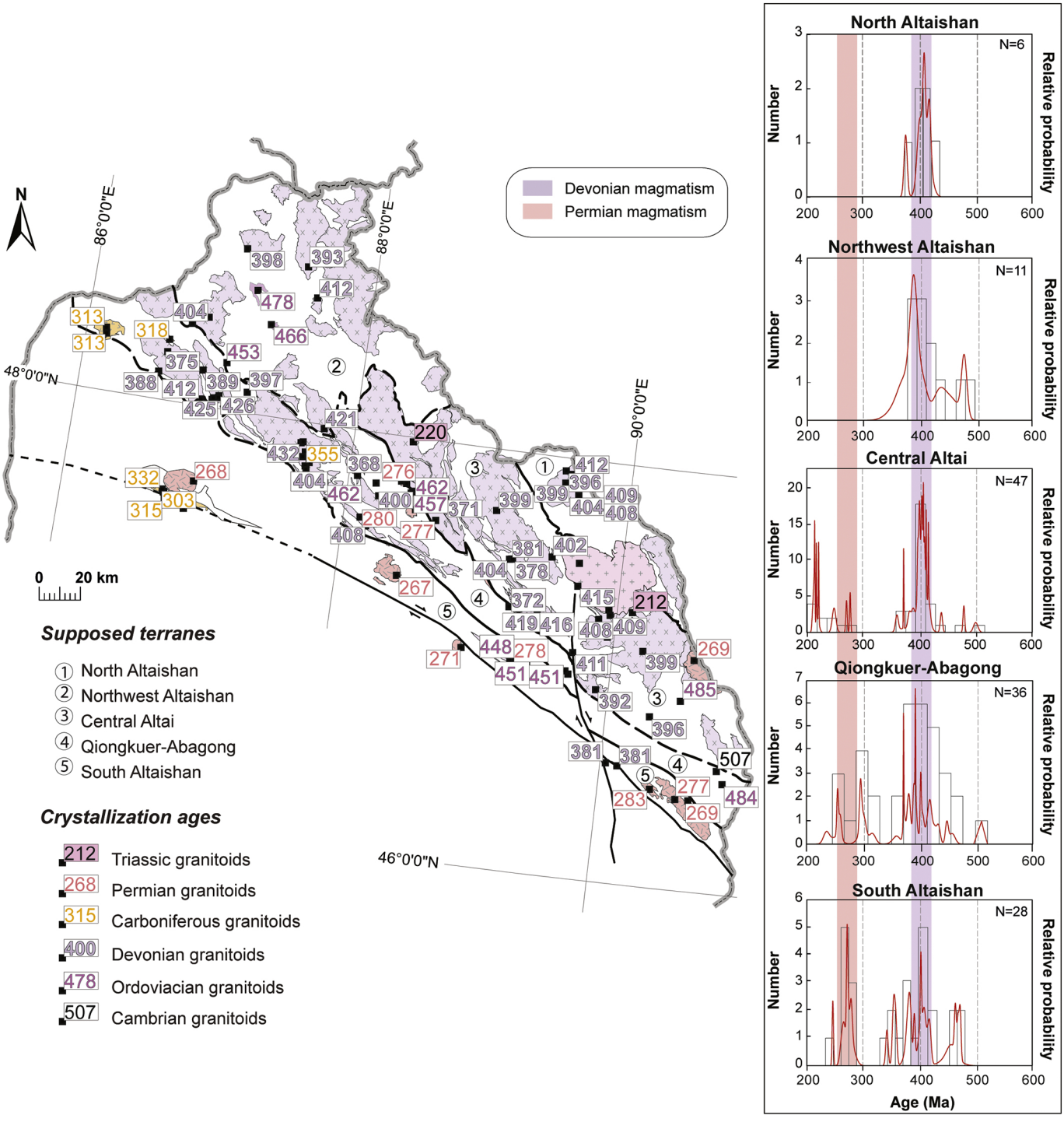
Devonian magmatism
Permian magmatism
N
86°0'0"E
88°0'0"E
90°0'0"E
48°0'0"N
46°0'0"N
0 20 km
Supposed terranes
① North Altaishan
② Northwest Altaishan
③ Central Altai
④ Qiongkuer-Abagong
⑤ South Altaishan
Crystallization ages
212 Triassic granitoids
268 Permian granitoids
315 Carboniferous granitoids
400 Devonian granitoids
478 Ordoviacian granitoids
507 Cambrian granitoids
North Altaishan
N=6
Northwest Altaishan
N=11
Central Altai
N=47
Qiongkuer-Abagong
N=36
South Altaishan
N=28
Number
Relative probability
Age (Ma)

Figure 7

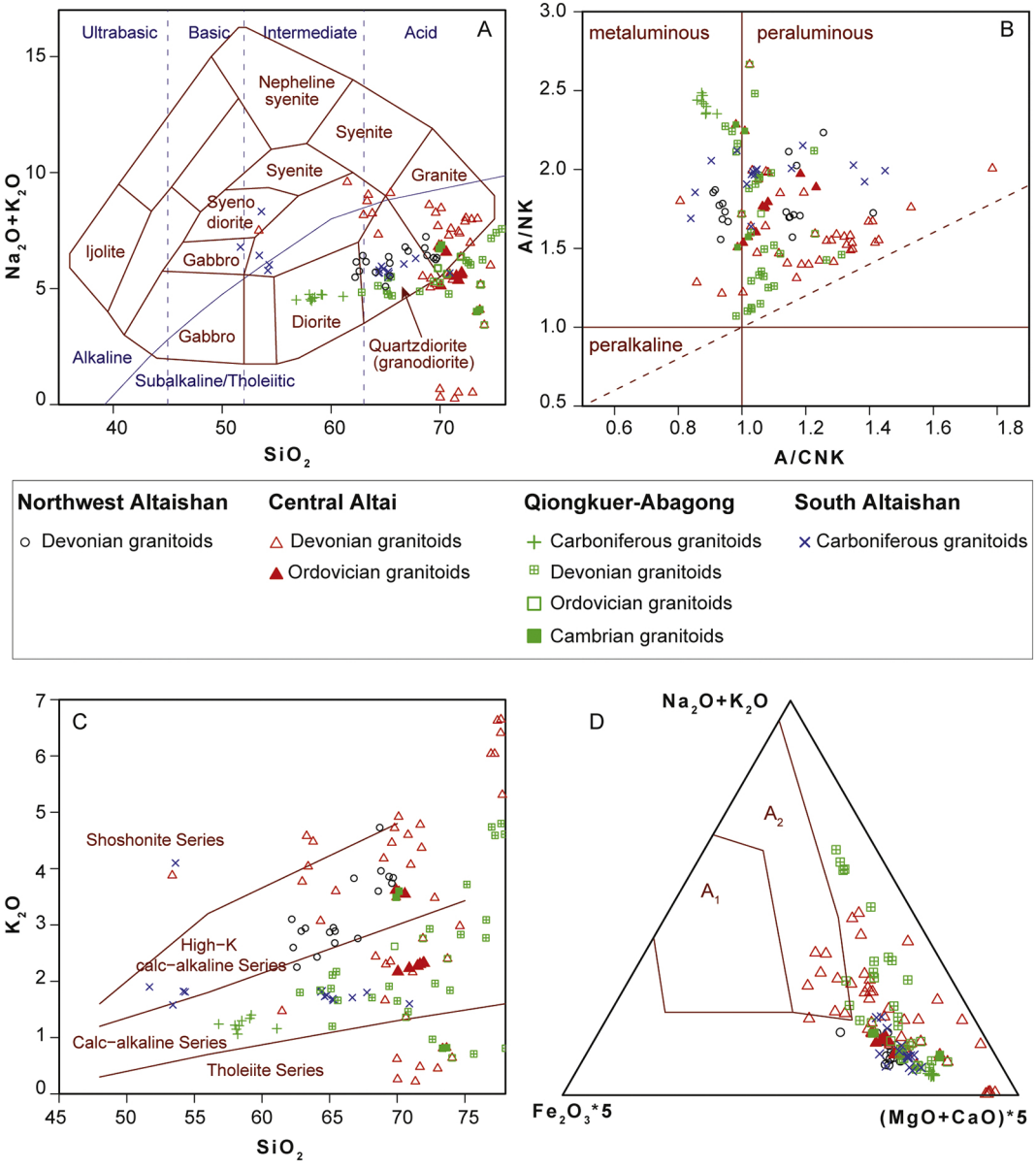
A
Ultrabasic
Basic
Intermediate
Acid
Nepheline syenite
Syenite
Syenite
Granite
Syenio diorite
Ijolite
Gabbro
Diorite
Gabbro
Alkaline
Subalkaline/Tholeiitic
Quartzdiorite (granodiorite)
Na2O+K2O
SiO2
B
metaluminous
peraluminous
peralkaline
A/NK
A/CNK
Northwest Altaishan
Devonian granitoids
Central Altai
Devonian granitoids
Ordovician granitoids
Qiongkuer-Abagong
Carboniferous granitoids
Devonian granitoids
Ordovician granitoids
Cambrian granitoids
South Altaishan
Carboniferous granitoids
C
Shoshonite Series
High-K calc-alkaline Series
Calc-alkaline Series
Tholeiite Series
K2O
SiO2
D
Na2O+K2O
A2
A1
Fe2O3*5
(MgO+CaO)*5

Figure 8

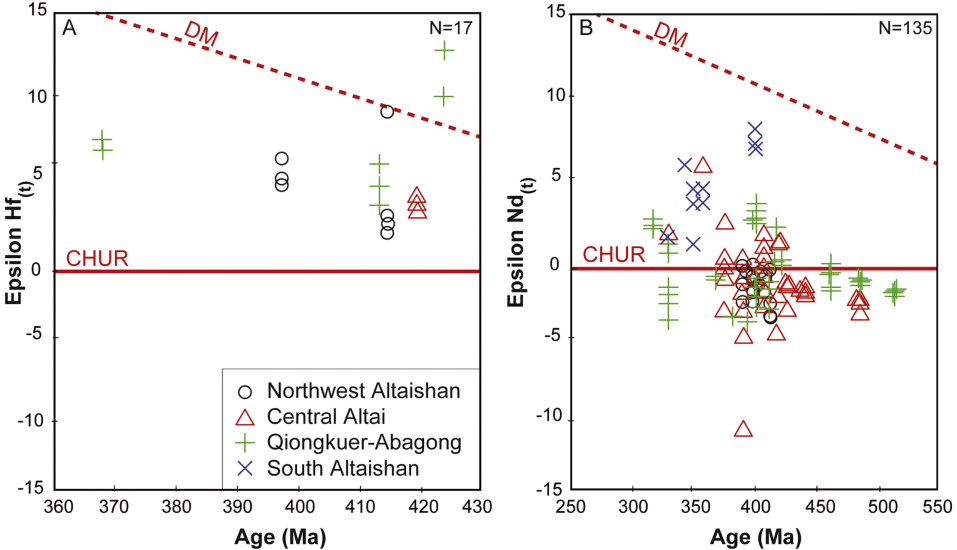
A
N=17
DM
CHUR
Epsilon Hf(t)
Age (Ma)
Northwest Altaishan
Central Altai
Qiongkuer-Abagong
South Altaishan
B
N=135
DM
CHUR
Epsilon Nd(t)
Age (Ma)

Figure 9

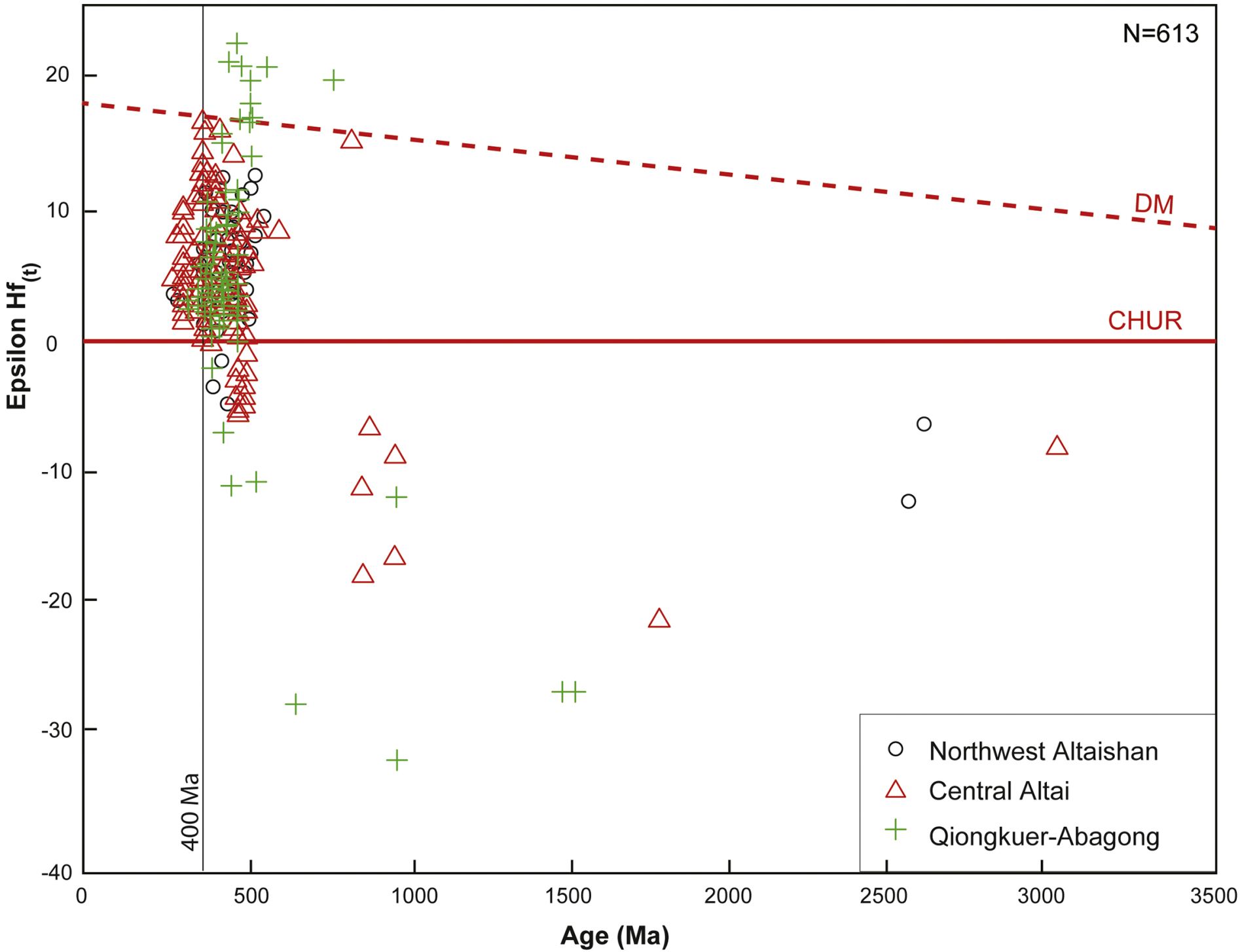
N=613
DM
CHUR
400 Ma
Epsilon Hf(t)
Age (Ma)
20
10
0
-10
-20
-30
-40
0
500
1000
1500
2000
2500
3000
3500
Northwest Altaishan
Central Altai
Qiongkuer-Abagong

Figure 10

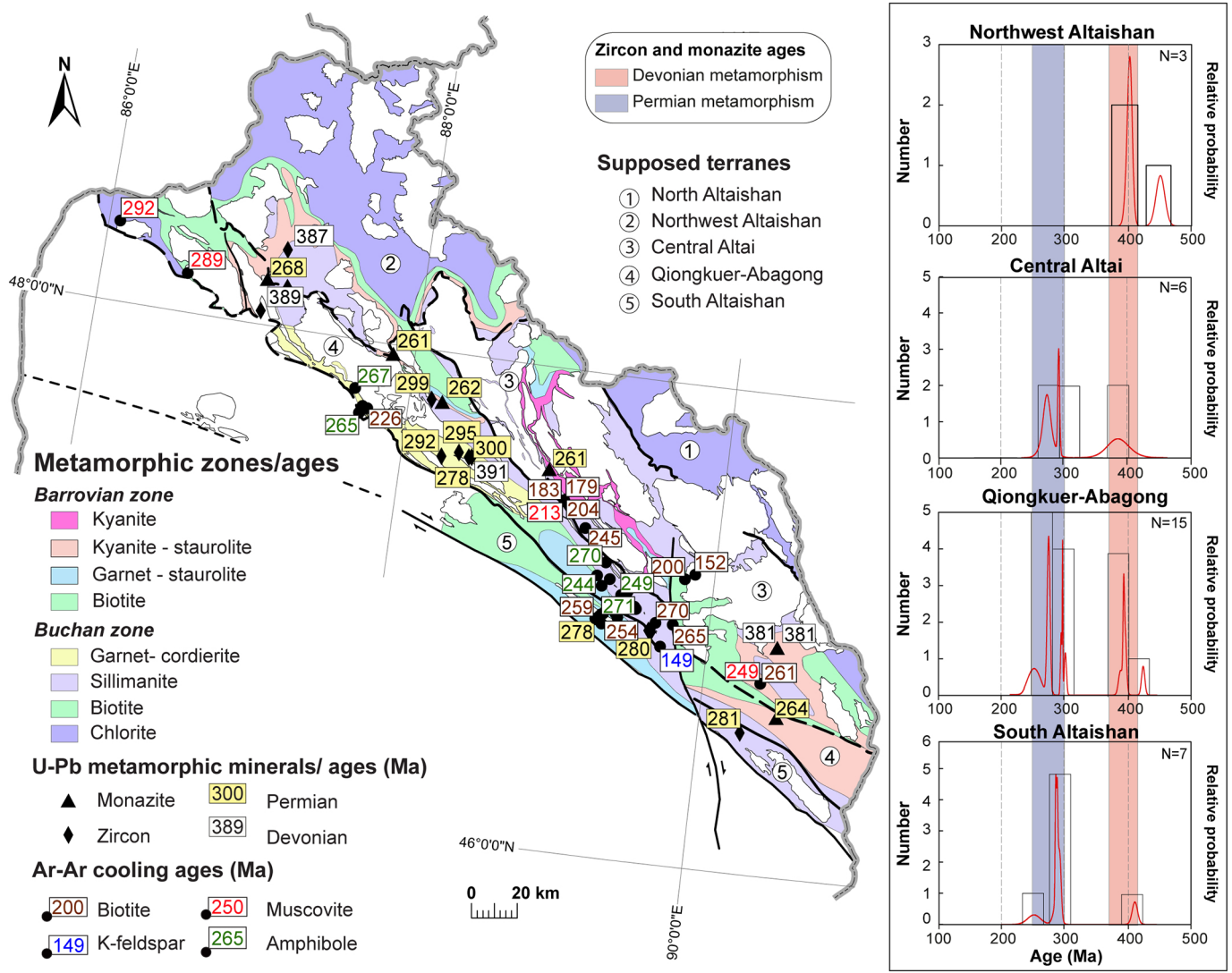
Zircon and monazite ages
Devonian metamorphism
Permian metamorphism
Supposed terranes
① North Altaishan
② Northwest Altaishan
③ Central Altai
④ Qiongkuer-Abagong
⑤ South Altaishan
Metamorphic zones/ages
Barrovian zone
Kyanite
Kyanite - staurolite
Garnet - staurolite
Biotite
Buchan zone
Garnet- cordierite
Sillimanite
Biotite
Chlorite
U-Pb metamorphic minerals/ ages (Ma)
Monazite
Zircon
300 Permian
389 Devonian
Ar-Ar cooling ages (Ma)
200 Biotite
149 K-feldspar
250 Muscovite
265 Amphibole
N
86°0'0"E
88°0'0"E
90°0'0"E
48°0'0"N
46°0'0"N
0 20 km
Northwest Altaishan
N=3
Central Altai
N=6
Qiongkuer-Abagong
N=15
South Altaishan
N=7
Number
Relative probability
Age (Ma)

Figure 11

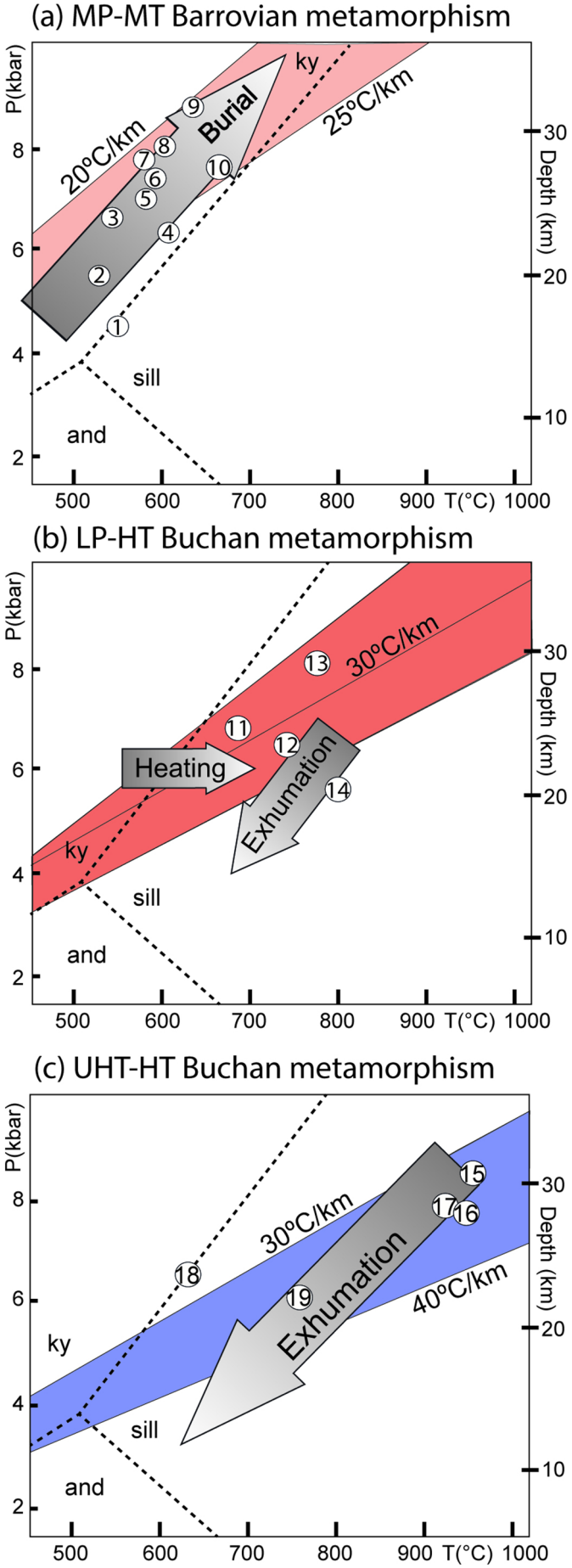
(a) MP-MT Barrovian metamorphism
P(kbar)
Depth (km)
T(°C)
20°C/km
25°C/km
Burial
ky
sill
and
1
2
3
4
5
6
7
8
9
10
(b) LP-HT Buchan metamorphism
30°C/km
Heating
Exhumation
ky
sill
and
11
12
13
14
(c) UHT-HT Buchan metamorphism
30°C/km
40°C/km
Exhumation
ky
sill
and
15
16
17
18
19

Figure 12

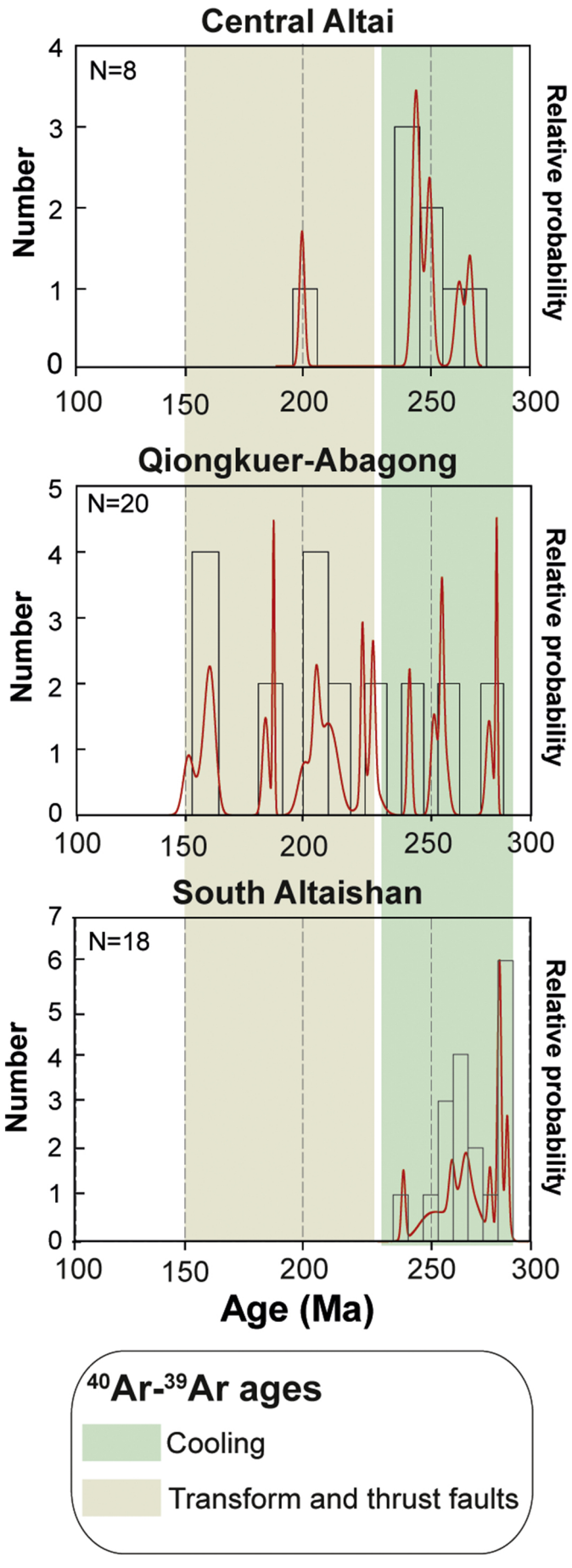
Central Altai
N=8
Number
Relative probability
Qiongkuer-Abagong
N=20
Number
Relative probability
South Altaishan
N=18
Number
Relative probability
Age (Ma)
40Ar-39Ar ages
Cooling
Transform and thrust faults

Figure 13

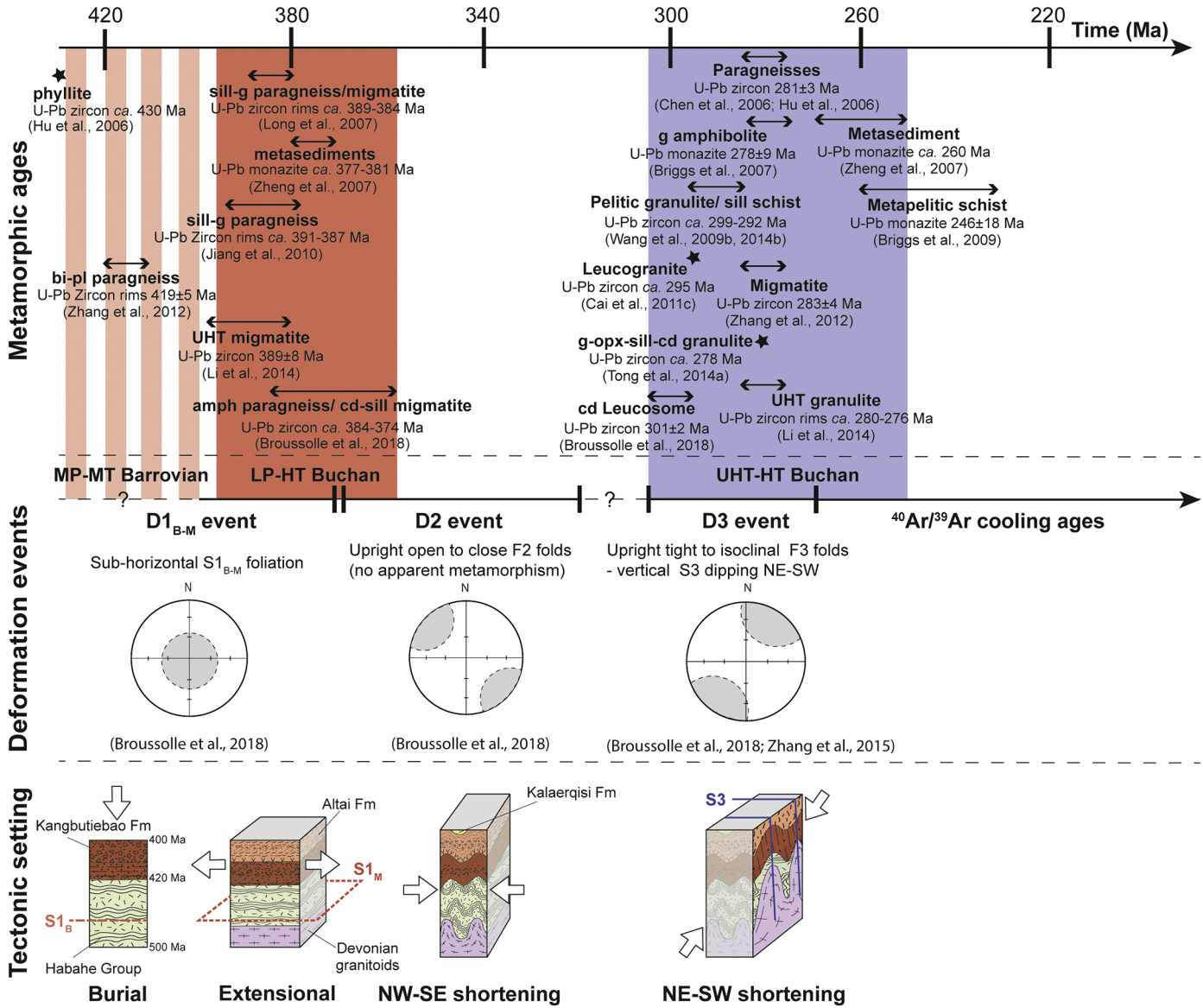
420
380
340
300
260
220
Time (Ma)
Metamorphic ages
phyllite
U-Pb zircon ca. 430 Ma
(Hu et al., 2006)
sill-g paragneiss/migmatite
U-Pb zircon rims ca. 389-384 Ma
(Long et al., 2007)
metasediments
U-Pb monazite ca. 377-381 Ma
(Zheng et al., 2007)
sill-g paragneiss
U-Pb Zircon rims ca. 391-387 Ma
(Jiang et al., 2010)
bi-pl paragneiss
U-Pb Zircon rims 419±5 Ma
(Zhang et al., 2012)
UHT migmatite
U-Pb zircon 389±8 Ma
(Li et al., 2014)
amph paragneiss/ cd-sill migmatite
U-Pb zircon ca. 384-374 Ma
(Broussolle et al., 2018)
Paragneisses
U-Pb zircon 281±3 Ma
(Chen et al., 2006; Hu et al., 2006)
g amphibolite
U-Pb monazite 278±9 Ma
(Briggs et al., 2007)
Metasediment
U-Pb monazite ca. 260 Ma
(Zheng et al., 2007)
Pelitic granulite/ sill schist
U-Pb zircon ca. 299-292 Ma
(Wang et al., 2009b, 2014b)
Metapelitic schist
U-Pb monazite 246±18 Ma
(Briggs et al., 2009)
Leucogranite
U-Pb zircon ca. 295 Ma
(Cai et al., 2011c)
Migmatite
U-Pb zircon 283±4 Ma
(Zhang et al., 2012)
g-opx-sill-cd granulite
U-Pb zircon ca. 278 Ma
(Tong et al., 2014a)
cd Leucosome
U-Pb zircon 301±2 Ma
(Broussolle et al., 2018)
UHT granulite
U-Pb zircon rims ca. 280-276 Ma
(Li et al., 2014)
MP-MT Barrovian
LP-HT Buchan
UHT-HT Buchan
?
?
D1B-M event
D2 event
D3 event
40Ar/39Ar cooling ages
Deformation events
Sub-horizontal S1B-M foliation
N
(Broussolle et al., 2018)
Upright open to close F2 folds
(no apparent metamorphism)
N
(Broussolle et al., 2018)
Upright tight to isoclinal F3 folds
- vertical S3 dipping NE-SW
N
(Broussolle et al., 2018; Zhang et al., 2015)
Tectonic setting
Kangbutiebao Fm
400 Ma
420 Ma
500 Ma
S1B
Habahe Group
Altai Fm
S1M
Devonian
granitoids
Kalaerqisi Fm
S3
Burial
Extensional
NW-SE shortening
NE-SW shortening

Figure 14

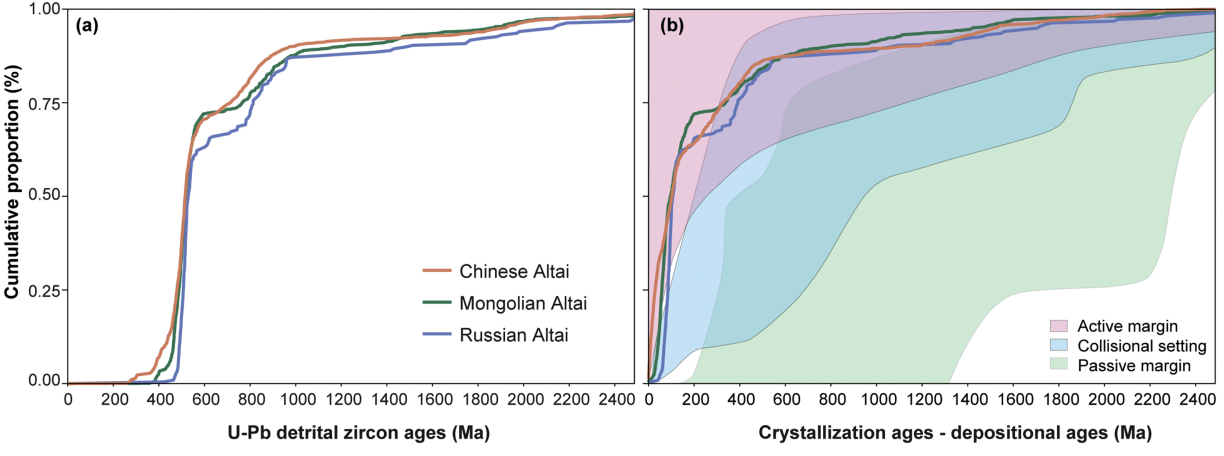
(a)
(b)
Cumulative proportion (%)
1.00
0.75
0.50
0.25
0.00
0 200 400 600 800 1000 1200 1400 1600 1800 2000 2200 2400
U-Pb detrital zircon ages (Ma)
Chinese Altai
Mongolian Altai
Russian Altai
Crystallization ages - depositional ages (Ma)
Active margin
Collisional setting
Passive margin

Figure 15

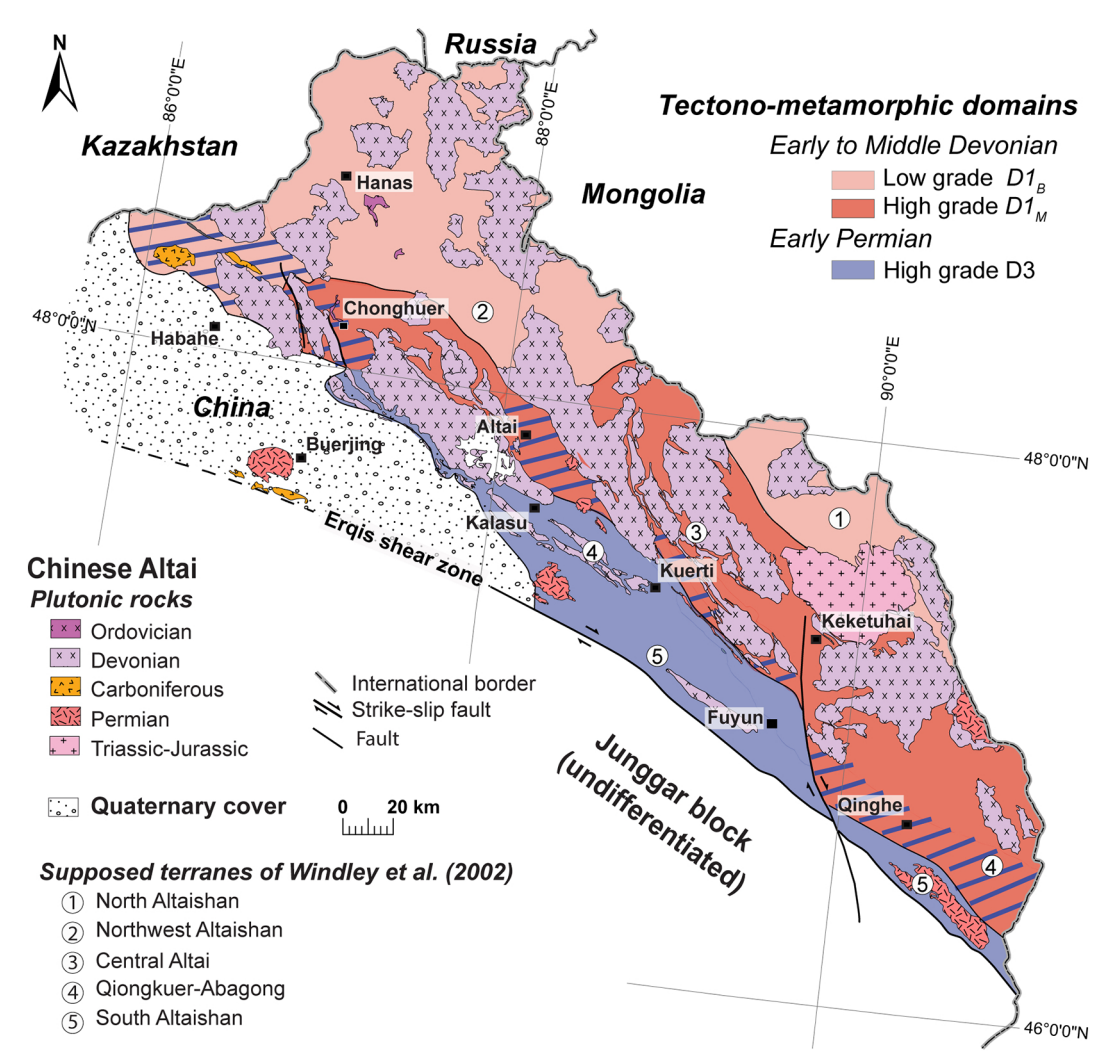
N
Russia
Kazakhstan
Mongolia
China
Hanas
Chonghuer
Habahe
Altai
Buerjing
Kalasu
Kuerti
Keketuhai
Fuyun
Qinghe
Erqis shear zone
86°0'0"E
88°0'0"E
90°0'0"E
48°0'0"N
46°0'0"N
Tectono-metamorphic domains
Early to Middle Devonian
Low grade $D1_B$
High grade $D1_M$
Early Permian
High grade D3
Chinese Altai
Plutonic rocks
Ordovician
Devonian
Carboniferous
Permian
Triassic-Jurassic
Quaternary cover
International border
Strike-slip fault
Fault
0 20 km
Junggar block (undifferentiated)
Supposed terranes of Windley et al. (2002)
1 North Altaishan
2 Northwest Altaishan
3 Central Altai
4 Qiongkuer-Abagong
5 South Altaishan

Figure 16